**Calhoun: The NPS Institutional Archive**

**DSpace Repository**

Theses and Dissertations | 1. Thesis and Dissertation Collection, all items

2014-06

# Mobile CubeSat Command and Control (MC3) 3-meter dish calibration and capabilities

Alcaide, Sarah M.

Monterey, California: Naval Postgraduate School

http://hdl.handle.net/10945/42572

This publication is a work of the U.S. Government as defined in Title 17, United States Code, Section 101. Copyright protection is not available for this work in the United States.

*Downloaded from NPS Archive: Calhoun*

http://www.nps.edu/library

Calhoun is the Naval Postgraduate School's public access digital repository for research materials and institutional publications created by the NPS community. Calhoun is named for Professor of Mathematics Guy K. Calhoun, NPS's first appointed -- and published -- scholarly author.

Dudley Knox Library / Naval Postgraduate School
411 Dyer Road / 1 University Circle
Monterey, California USA 93943

# NAVAL POSTGRADUATE SCHOOL

**MONTEREY, CALIFORNIA**

# THESIS

**MOBILE CUBESAT COMMAND AND CONTROL (MC3)
3-METER DISH CALIBRATION AND CAPABILITIES**

by

Sarah M. Alcaide

June 2014

Thesis Advisor: James H. Newman
Second Reader: Jonathan S. Matey

**Approved for public release; distribution is unlimited**

THIS PAGE INTENTIONALLY LEFT BLANK

# REPORT DOCUMENTATION PAGE

*Form Approved OMB No. 0704-0188*

Public reporting burden for this collection of information is estimated to average 1 hour per response, including the time for reviewing instruction, searching existing data sources, gathering and maintaining the data needed, and completing and reviewing the collection of information. Send comments regarding this burden estimate or any other aspect of this collection of information, including suggestions for reducing this burden, to Washington headquarters Services, Directorate for Information Operations and Reports, 1215 Jefferson Davis Highway, Suite 1204, Arlington, VA 22202-4302, and to the Office of Management and Budget, Paperwork Reduction Project (0704-0188) Washington DC 20503.

| **1. AGENCY USE ONLY *(Leave blank)*** | **2. REPORT DATE** June 2014 | **3. REPORT TYPE AND DATES COVERED** Master's Thesis |
|---|---|---|

**4. TITLE AND SUBTITLE**
MOBILE CUBESAT COMMAND AND CONTROL (MC3) 3-METER DISH CALIBRATION AND CAPABILITIES

**5. FUNDING NUMBERS**

**6. AUTHOR(S)** Sarah M. Alcaide

**7. PERFORMING ORGANIZATION NAME(S) AND ADDRESS(ES)**
Naval Postgraduate School
Monterey, CA 93943-5000

**8. PERFORMING ORGANIZATION REPORT NUMBER**

**9. SPONSORING /MONITORING AGENCY NAME(S) AND ADDRESS(ES)**
N/A

**10. SPONSORING/MONITORING AGENCY REPORT NUMBER**

**11. SUPPLEMENTARY NOTES** The views expressed in this thesis are those of the author and do not reflect the official policy or position of the Department of Defense or the U.S. Government. IRB protocol number ____N/A____.

**12a. DISTRIBUTION / AVAILABILITY STATEMENT**
Approved for public release; distribution is unlimited

**12b. DISTRIBUTION CODE**
A

**13. ABSTRACT (maximum 200 words)**

The Mobile CubeSat Command and Control (MC3) architecture is a growing network of ground stations that spans the United States of America. It was designed to support the National Reconnaissance Office's Experimental CubeSat Program. Each node was originally designed to communicate via UHF and S-band frequencies using Yagi antenna only. The MC3 ground station at the Naval Postgraduate School has recently incorporated a 3-meter S-band dish. This thesis documents the calibration and capabilities of the new S-band dish. It also investigates the possibility of using the antenna outside of its normal operating range. In particular, the idea of using an S-band, 3-meter dish to receive UHF band signals was tested by designing a UHF signal feed optimized for 915 MHz and used to listen to a UHF source deployed on a high altitude balloon at near orbital distances. In addition, this document discusses the integration of a dish system into current and future MC3 ground stations.

| **14. SUBJECT TERMS** CubeSat, ground station, network, MC3 | | | **15. NUMBER OF PAGES** 85 |
|---|---|---|---|
| | | | **16. PRICE CODE** |
| **17. SECURITY CLASSIFICATION OF REPORT** Unclassified | **18. SECURITY CLASSIFICATION OF THIS PAGE** Unclassified | **19. SECURITY CLASSIFICATION OF ABSTRACT** Unclassified | **20. LIMITATION OF ABSTRACT** UU |

NSN 7540-01-280-5500

Standard Form 298 (Rev. 2-89)
Prescribed by ANSI Std. 239-18

THIS PAGE INTENTIONALLY LEFT BLANK

**Approved for public release; distribution is unlimited**

# MOBILE CUBESAT COMMAND AND CONTROL (MC3) 3-METER DISH CALIBRATION AND CAPABILITIES

Sarah M. Alcaide
Major, United States Marine Corps
B.S., Mary Baldwin College, 2001

Submitted in partial fulfillment of the
requirements for the degree of

**MASTER OF SCIENCE IN SPACE SYSTEM OPERATIONS**

from the

**NAVAL POSTGRADUATE SCHOOL**
**June 2014**

Author: Sarah M. Alcaide

Approved by: James H. Newman
Thesis Advisor

Jonathan S. Matey
Second Reader

Rudolf Panholzer
Chair, Space Systems Academic Group

THIS PAGE INTENTIONALLY LEFT BLANK

# ABSTRACT

The Mobile CubeSat Command and Control (MC3) architecture is a growing network of ground stations that spans the United States of America. It was designed to support the National Reconnaissance Office's Experimental CubeSat Program. Each node was originally designed to communicate via UHF and S-band frequencies using Yagi antenna only. The MC3 ground station at the Naval Postgraduate School has recently incorporated a 3-meter S-band dish. This thesis documents the calibration and capabilities of the new S-band dish. It also investigates the possibility of using the antenna outside of its normal operating range. In particular, the idea of using an S-band, 3-meter dish to receive UHF band signals was tested by designing a UHF signal feed optimized for 915 MHz and used to listen to a UHF source deployed on a high altitude balloon at near orbital distances. In addition, this document discusses the integration of a dish system into current and future MC3 ground stations.

THIS PAGE INTENTIONALLY LEFT BLANK

# TABLE OF CONTENTS


I. INTRODUCTION ..... 1
A. MOBILE CUBESAT COMMAND AND CONTROL BACKGROUND ..... 2
B. THESIS OBJECTIVES ..... 4

II. MC3 3-METER DISH INSTALLATION AND CALIBRATION ..... 5
A. INSTALLATION AND MODIFICATIONS ..... 5
1. Antenna Site ..... 5
2. Hardware ..... 6
3. Assembly ..... 7
4. Software ..... 9
5. Modification ..... 9
B. INITIAL POINTING CALIBRATION ..... 10
C. CONSTRAINTS ..... 11
D. LINK BUDGET ..... 13
E. SUMMARY ..... 15

III. MC3 3-METER DISH CAPABILITIES TESTING ..... 17
A. NEARBY HILLTOP TESTING ..... 17
1. Purpose ..... 17
2. Method ..... 17
3. Test Locations ..... 18
4. Equipment ..... 19
5. Hilltop Test Procedure ..... 20
6. Results ..... 21
B. HIGH ALTITUDE BALLOON TEST S-BAND ..... 24
1. Project Stratosphere ..... 24
2. Purpose of the S-band HAB Flight ..... 24
3. HAB Communications Payload ..... 25
*a. BBB Single Board Computer ..... 26*
*b. GPS Receivers ..... 27*
*c. Automatic Packet Reporting System ..... 27*
*d. SPOT Tracker ..... 27*
4. Location of Balloon Release ..... 28
5. Procedure for HAB Communications ..... 29
6. Results ..... 32
C. SCAN TESTBED ..... 33
1. SDRs aboard the ISS ..... 34
2. Testing Proposal ..... 35
3. Testing Equipment at NPS ..... 36
4. Procedure for SCaN Testbed Experiment ..... 37
5. Results ..... 37
D. HAB TEST WITH UHF FEED MODIFICATION OF DISH SYSTEM ..... 40
1. Directed Study ..... 40

2. Components of the HAB Payload ..... 41
*a. BBB Single Board Computer ..... 42*
*b. GPS Receivers ..... 42*
*c. Automatic Packet Reporting System ..... 42*
*d. SPOT Tracker ..... 43*
3. Component Interaction ..... 43
4. Communication Operations ..... 44
5. 3-Meter Dish Modification ..... 45
*a. Creation of the UHF Feed ..... 45*
6. Flight Path Predication ..... 52
7. Procedure for Communications ..... 53
8. Results ..... 54
E. SUMMARY ..... 56
IV. CONCLUSION AND FUTURE WORK ..... 57
A. CONCLUSION ..... 57
B. FUTURE WORK ..... 58
1. Keyhole Constraint ..... 58
2. UHF Feed on Dish Assembly ..... 58
3. Performance Characteristics ..... 58
4. Summary ..... 59
APPENDIX A. MHX TEST MESSAGES ..... 61
APPENDIX B. HAB MHX-2400 MESSAGES RECEIVED BY 3-METER DISH FROM 20:09 TO 20:13 ON DECEMBER 21, 2013 ..... 63
LIST OF REFERENCES ..... 65
INITIAL DISTRIBUTION LIST ..... 67

# LIST OF FIGURES


Figure 1. MC3 VPN CONOPS, from [2] ..... 3
Figure 2. 3-meter dish system location at NPS ..... 6
Figure 3. 3-meter dish system hardware ..... 7
Figure 4. Dish feed assembly and electrical housing integration ..... 8
Figure 5. Satellite Ground Station Lab at NPS ..... 9
Figure 6. Spot elevations around the 3-meter dish system ..... 12
Figure 7. MHX radio testing locations ..... 18
Figure 8. MHX-2400 development kit, from [6] ..... 19
Figure 9. Mobile MHX-2400 radio system used for field testing ..... 20
Figure 10. S-band HAB payload testing at NPS ..... 26
Figure 11. BBB ..... 26
Figure 12. GPS receiver ..... 27
Figure 13. SPOT tracker ..... 28
Figure 14. HAB flight prediction for December 21, 2013 ..... 29
Figure 15. S-band HAB inflation ..... 31
Figure 16. S-band HAB release ..... 31
Figure 17. SCaN Testbed system overview, from [12] ..... 34
Figure 18. SCaN Testbed major components viewed from ram/zenith angle (stowed position shown), from [12] ..... 35
Figure 19. ETTUS SDR, from [19] ..... 36
Figure 20. ETTUS specifications, from [19] ..... 37
Figure 21. FFT plot of first pass of SCaN Testbed on January 22, 2014 ..... 39
Figure 22. FFT Plot of second pass of SCaN Testbed on January 22, 2014 ..... 39
Figure 23. FFT plot of SCaN contact on January 24, 2014 ..... 40
Figure 24. APRS transceiver ..... 43
Figure 25. Conceptual diagram of HAB component interaction ..... 44
Figure 26. First 915 MHz single helix antenna, 4NEC2 model ..... 48
Figure 27. SWR graph of first 915 MHz antenna ..... 48
Figure 28. 915 MHz single helix antenna, 4NEC2 model ..... 50
Figure 29. SWR graph of final 915 MHz antenna ..... 51
Figure 30. 915 MHz antenna feed for 3-meter parabolic dish ..... 51
Figure 31. Spectrum analyzer test of final UHF feed antenna ..... 52
Figure 32. Predicted and actual flight path of directed study HAB, from [11] ..... 53

THIS PAGE INTENTIONALLY LEFT BLANK

# LIST OF TABLES


Table 1. MC3 antennae specifications, from [2] ..... 4
Table 2. Sample link budget for S-band dish system and SCAT, from [9] ..... 14
Table 3. MHX-2400 testing results from nearby hilltops ..... 21
Table 4. Estimated Link Margin Calculator ..... 22
Table 5. RSSI values for MHX-2400 HAB flight ..... 32
Table 6. Schedule of passes for SCaN Testbed experiments ..... 38
Table 7. First UHF helical antenna design details from jcoppens.com ..... 47
Table 8. Design performance of first 915 MHz antenna ..... 48
Table 9. Final UHF helical antenna design details, from [16] ..... 49
Table 10. Final 915 MHz antenna design parameters and results ..... 50
Table 11. NPS 3-meter dish GDP measurements, from [11] ..... 55
Table 12. NPS MC3 Yagi antenna GDP measurements, from [11] ..... 55

THIS PAGE INTENTIONALLY LEFT BLANK

# LIST OF ACRONYMS AND ABBREVIATIONS

| | |
|---|---|
| AFIT | Air Force Institute of Technology |
| APRS | Automatic Packet Reporting System |
| AstroDev | Astro devices |
| BBB | Beagle-Bone Black |
| BPTF | Blossom Point Tracking Facility |
| BRM | Balloon release mechanism |
| C2 | Command and control |
| C2B | Colony II Bus |
| CGA | Common ground architecture |
| CONOPS | Concept of operations |
| COTS | Commercial off-the-shelf |
| CW | Continuous wave |
| dBci | Decibels isotropic circular |
| dBm | Decibel-milliwatts |
| DOD | Department of Defense |
| eMC3 | Experimental Mobile CubeSat Command and Control |
| FFT | Fast Fourier transform |
| GOTS | Government off-the-shelf |
| HAB | High altitude balloon |
| hrMC3 | High-Reliability Mobile CubeSat Command and Control |
| HSFL | Hawaii Spaceflight Laboratory |
| ISS | International Space Station |
| ITU | International Telecommunication Union |
| JPL | Jet Propulsion Laboratory |
| KBR | Kevin Brown Radio |
| LEO | Low earth orbit |
| MC3 | Mobile CubeSat command and control |
| NASA | National Aeronautics and Space Administration |
| NMEA | National Marine Electronics Association |
| NPS | Naval Postgraduate School |

| | |
|---|---|
| NRL | Naval Research Laboratory |
| NRO | National Reconnaissance Office |
| RSSI | Received signal strength indicator |
| SCaN | Space communications and navigation |
| SDL | Space Dynamics Laboratory |
| SDR | Software-defined radio |
| SmallSat | Small satellite |
| SOC | Satellite Operations Center |
| SPOT | Satellite position and tracking |
| SRI | Stanford Research Institute |
| SSAG | Space Systems Academic Group |
| STRS | Space Telecommunications Radio System |
| SWR | Standing wave ratio |
| TDRSS | Tracking and Data Relay Satellite System |
| UART | Universal Asynchronous Receiver/Transmitters |
| UHF | Ultra high frequency |
| USU | Utah State University |
| UTC | Coordinated universal time |
| VPN | Virtual private network |

# ACKNOWLEDGMENTS

First and foremost, I would like to express my sincere gratitude to my thesis advisor, Dr. James Newman, and my second reader, LTC Scott Matey, for their patient guidance and encouragement. Their knowledge, enthusiasm and support, along with their participation in lab experiments, were instrumental in the completion of this thesis.

I would also like to thank the SmallSat lab personnel. David Rigmaiden patiently answered all of my questions about lab equipment and experimentation. I am especially thankful for his assistance with the UHF feed for the 3-meter dish assembly. In addition, I am thankful for the time and assistance given by Dan Sakoda to create the 3D form used by the UHF feed. I am forever indebted to Giovanni Minelli, Aaron Felt, James Horning, and Natasha Nogueira for their professionalism, guidance, and assistance in experiments throughout my time in the SmallSat lab. In addition, I would like to thank my classmates, Maj. Dwain Donaldson, Capt. Patrick Schrafft, and Capt. Clayton Jarolimek, for participating in the HAB flight.

I am also appreciative of the incredible love, encouragement and prayers of my family and friends.

I give the most heartfelt thanks to my husband and best friend, Yourdy, and my daughter, Keyra. Without their remarkable love, patience, kindness and understanding, the completion of this thesis would not be possible. I am especially grateful for the endless laughter and encouragement they bring to my life.

Finally, I would like to thank God for all the blessings he has given my family before and during my work on this thesis.

THIS PAGE INTENTIONALLY LEFT BLANK

# I. INTRODUCTION

Satellites come in a variety of shapes and sizes. They each have a unique purpose, such as communications or remote sensing, and are utilized by militaries, commercial companies and universities worldwide. In the current fiscally constrained environment, smaller satellites are becoming highly desirable for research and operations. Emerging technologies are enabling very small satellites to become more versatile and capable. One of the more common very small satellites is termed the CubeSat [1]. CubeSats are frequently used to conduct scientific experiments and increase the technology readiness levels of satellite systems. Currently, CubeSats are used for remote sensing, atmospheric studies, communications, biology studies, space weather studies and several other purposes [1]. As the number of CubeSats on orbit increases, ground networks must be established to handle their communication and data flow.

The Mobile CubeSat Command and Control (MC3) ground stations were created as a network to support experimental, U.S. government CubeSats. The ground station nodes are fully automated and can be controlled locally and remotely. They also create a unique learning environment and provide a common ground for partnership between government and civilian institutions [2].

Communication with CubeSats has commonly been via ultra high frequencies (UHF). Currently, there is a movement to shift from UHF downlink communication to S-band downlink communication to increase the data throughput from orbit. The MC3 ground stations are all equipped to handle S-Band communications through the use of Yagi antennae. Table 1 outlines the specifications for each of these resources. The node located at the Naval Postgraduate School (NPS) has incorporated an additional 3-meter S-band dish. Once the calibration and capabilities have been explored, this S-Band dish could become a standard addition to MC3 nodes. This evolution of the MC3 architecture highlights the adaptability of the system and ensures that the MC3 ground stations remain an asset for future CubeSat missions.

## A. MOBILE CUBESAT COMMAND AND CONTROL BACKGROUND

MC3 ground stations were originally developed by the Naval Research Laboratory (NRL) to be the ground architecture for the NRO Colony CubeSat Program [3]. The nodes within MC3 will support the Colony CubeSats, which are equipped with the standardized Colony II Bus (C2B), by supplying communications via an 450 MHz uplink and a 915 MHz downlink [2]. Detailed information on MC3 is available in Lieutenant Philip Ibbittson's thesis, "Mobile CubeSat Command and Control architecture and CONOPS" [2]. NRL designed the architecture using Commercial Off-the-Shelf (COTS) hardware and Government Off-the-Shelf (GOTS) software [5]. Operational control of MC3 was divided between two locations. NPS was established as the Satellite Operations Center (SOC) for experimental CubeSat missions. The NRL Blossom Point Tracking Facility (BPTF) is the SOC for operational or high-reliability CubeSat missions.

The experimental MC3 (eMC3), as distinct from the high reliability MC3 (hrMC3), ground architecture stretches across the United States of America. Currently, there are ground stations located at the Hawaii Spaceflight Laboratory (HSFL) at the University of Hawaii in Honolulu, Hawaii, the Air Force Institute of Technology (AFIT) in Dayton, Ohio, the Space Dynamics Laboratory (SDL) at Utah State University (USU) in Logan, Utah, the University of New Mexico in Albuquerque, NM, and NPS in Monterey, California [4]. In the future, other ground stations may be incorporated to increase the coverage area of the network. Transportable Yagi antennae and communication racks make eMC3 nodes possible in almost any location. This could be a benefit to the Department of Defense (DOD) if a need to command and control experimental CubeSats exists in the future.

All eMC3 ground stations use a version of the NRL's common ground architecture (CGA) software, known as Neptune, and are connected by a virtual private network (VPN). The Neptune software was created, and is maintained, by NRL to handle spacecraft testing and on orbit operations. To schedule

communication with an experimental spacecraft, satellite users send a request to NPS. Then Neptune software is used by MC3 personnel to schedule requested communications. Next, Neptune software can automatically or manually be used to task resources inside the MC3 network. The MC3 network works in an unclassified environment, but it can certainly pass along encrypted payload or other telemetry files to any user. This highlights another benefit to potential DOD users in need of a ground network capable of handling encrypted information of any classification. Figure 1 shows the VPN concept of operations (CONOPS) for MC3, from [2].

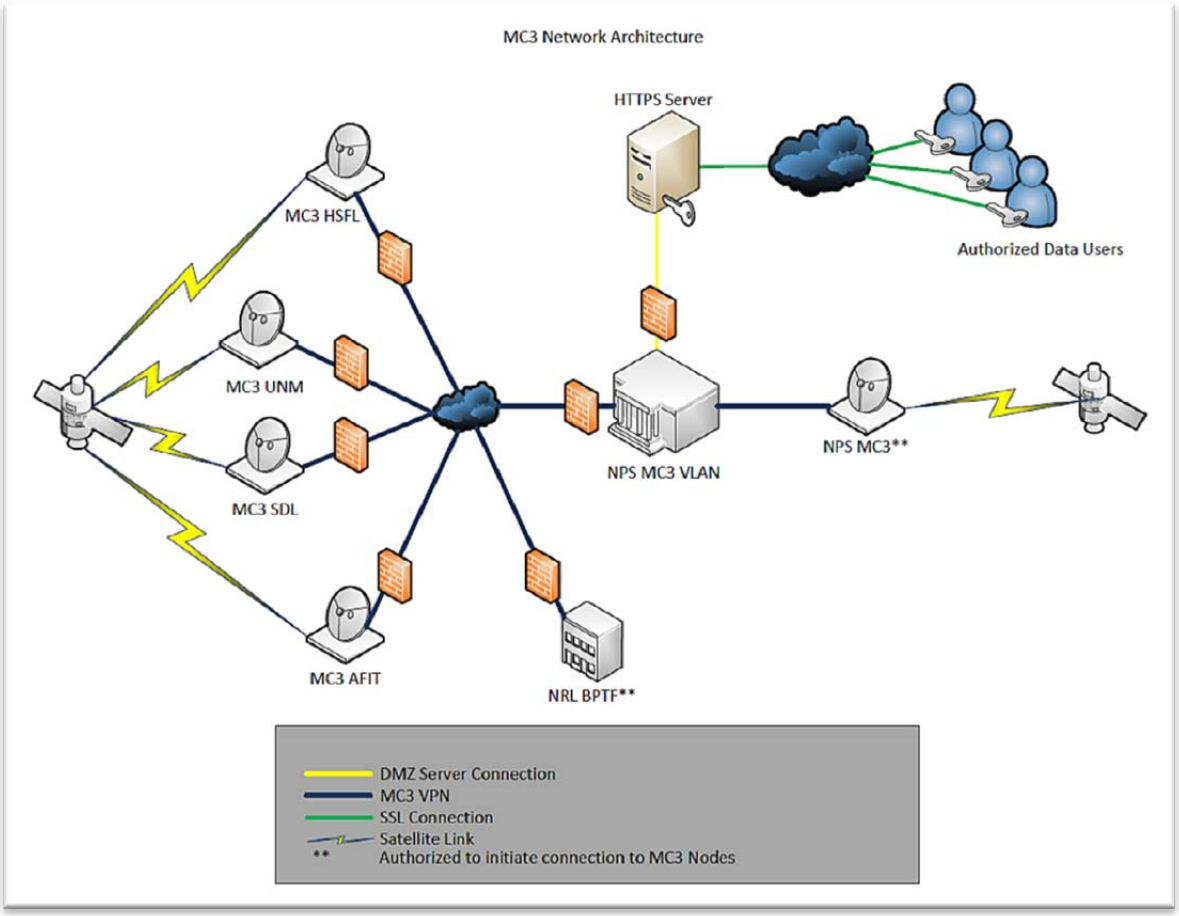


Figure 1. MC3 VPN CONOPS, from [2]

Table 1 displays the performance characteristics of the UHF Yagis, the S-band Yagi, and the 3-meter dish antennas. It also descrbes the attributes of the rotators associated with each antenna and its receiver.

| Antennas | UHF TX YAGI | UHF RX YAGI | SBAND TX YAGI | SBAND RX YAGI | SBAND 3m DISH |
|---|---|---|---|---|---|
| Model # | M² 450CP28 | 4 x M² 917Y | M² 1975-23 | M² 2227-21 | M² Parabolic, Custom |
| Frequency Range | 435-455 MHz | 880-940 MHz | 1925-2075 MHz | 2210-2245 MHz | 1.8-4.0 GHz (est.) |
| Beamwidth | 28° Circular | | E =26°, H = 28° | E=13°, H = 13° | 3° @ 2.1 GHz (est.) |
| Gain (dBi) | 16.0 | 18.5 | 17.25 | 21 | 33 @ 2.1 GHz (est.) |
| TX Power (W) | 75 | | 30 | | 30 |
| EIRP (dbW) | 31.7 | | 29.02 | | 51.75 |

| Receiver | | Rotators | YAGIs | 3m DISH |
|---|---|---|---|---|
| Model # | GDP 4425D | Model # | Yaesu G-5500 | M² AZEL 1000S |
| Range, Ch1 (MHz) | 2185-2485, 1700-1850, 1427-1545 | Rate (El/ Az deg/sec) | 2.7/ 6.2 | 8.0/ 8.0 |
| Range, Ch2 (MHz) | 902-918 | Accuracy | ± 4% | ± 0.02° |
| Demodulation | FSK, BPSK, QPSK, OQPSK, GMSK | | | |
| Noise Figure | < 10dB | | | |
| Dynamic Range | > 90dB | | | |

Table 1. MC3 antennae specifications, from [2]

## B. THESIS OBJECTIVES

One objective of this thesis is to document the installation and calibration of the MC3 S-band dish system. Another goal is to validate the capabilities of the dish system through testing. The experiments the author was involved in include a test to increase the slew rate of the dish system, local hilltop testing with an MHX-2400 radio, communications testing with NASA's Space Communications and Navigation (SCaN) Testbed and High Altitude Balloon (HAB) experiments. This thesis also investigates the possibility of using the dish antenna outside of its normal operating range. To meet this goal, the author designed a UHF feed antenna for the dish system optimized for 915 MHz and then used it to listen to a UHF source deployed on a high altitude balloon at near orbital distances.

# II. MC3 3-METER DISH INSTALLATION AND CALIBRATION

To maximize the benefits of the three-meter, S-band dish system, a site survey and proper installation and calibration must be conducted. Then the limitations of the system must be characterized and proper allowances for those limitations made during antenna operations.

## A. INSTALLATION AND MODIFICATIONS

### 1. Antenna Site

Several factors must be considered when conducting a site survey for any dish system. The climate, elevation and physical obstructions around potential sites are among the first concerns. In many cases, rooftops are the best option because of their height and stability. Depending on the location, a protective antenna dome may be necessary if snow, strong winds or heavy foliage are common in the area. The size of the antenna dome or the frame used to mount the dish assembly becomes the deciding factor on the required size of the antenna site.

The roof of Spanagel Hall at NPS was chosen as the suitable location for this 3-meter dish system. This site, the highest location on campus, is where most of NPS's communications antennas are located. From this location, the antennas are unobstructed by buildings or towering redwoods that are common on campus. It is also within a relatively short distance from the Small Satellite (SmallSat) lab and MC3 control room. Figure 2 shows the configuration of the 3-meter dish system at NPS. Because Monterey, California, has consistently mild weather, a dome to house the antenna and frame was not necessary.

Figure 2. 3-meter dish system location at NPS

## 2. Hardware

The MC3 dish antenna and rotors were procured from M2 Antenna Systems Inc. The 3-meter parabolic dish system is advertised as having higher gain, better pointing accuracy and faster slew rates than the Yagi antennas [6]. Table 1 displays its advertised performance in each of those areas. The dish is fitted with an S-band feed and a custom-built UHF feed assembly. The creation of the UHF feed assembly is discussed in Chapter III, Section D of this document.

The primary receiver for the dish system is a two channel GDP Space Systems G4425D Software-defined radio (SDR) (Table 1). Four antennas (two UHF and two L-band or S-band antennas) can be connected to this receiver at once. Of note, the GDP is capable of switching operations between antennas through remote access.

The base for the antenna was custom built by SmallSat engineers. The engineers started with an existing frame from a decommissioned antenna on the roof of Spanagel Hall. That frame was modified to house a 6 inch pipe required to mount the new antenna. To complete the structure, SmallSat engineers machined unique support poles to further steady the 6-inch pipe. The individual parts of the dish system are labelled in Figure 3.

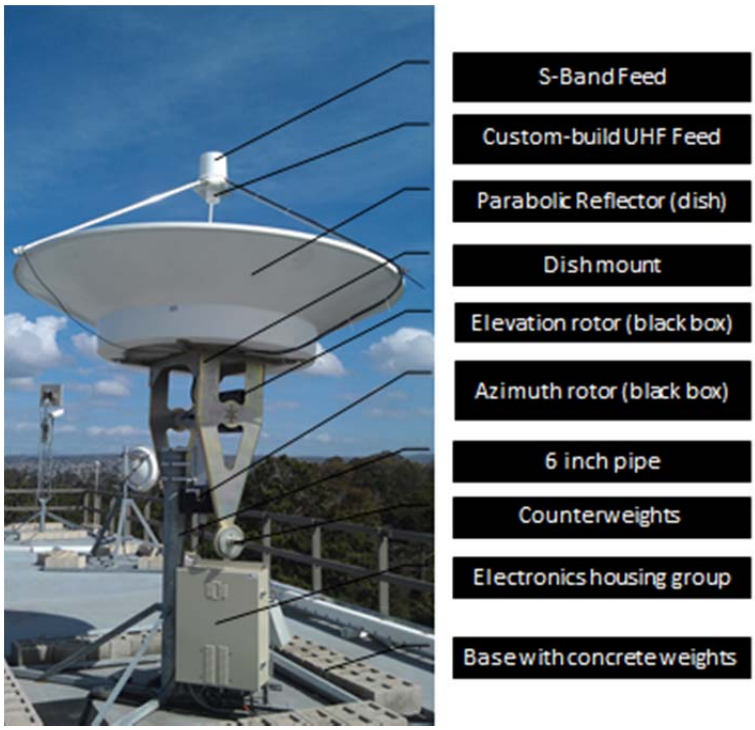


Figure 3. 3-meter dish system hardware

## 3. Assembly

Assembly of the dish system at NPS was completed over several months as time and personnel were available. It is possible for assembly to be accomplished in approximately one week if dedicated resources and time are available. Construction of the antenna began by transporting the individual parts via forklift to Spanagel Hall. Then cranes located on the roof were used to hoist each part into position. The SmallSat Team utilized the instruction manual from M2 Antenna Systems to assemble the dish and rotors.

Once erected, concrete weights were placed around the base of the dish system to further stabilize it. Next, the feed and electronic housing were assembled and tested in the lab and subsequently attached to the antenna frame. Finally, cabling to connect the dish system to the MC3 node was incorporated. Figure 4 shows the dish feed construction in the SmallSat lab and electronics housing integration at the antenna site. NPS was able to achieve thousands of dollars in cost savings by utilizing SmallSat personnel to assemble the dish system and creating a base for the antenna from existing hardware. Cost saving were also attained because the antenna did not require a dome for protection against the elements.

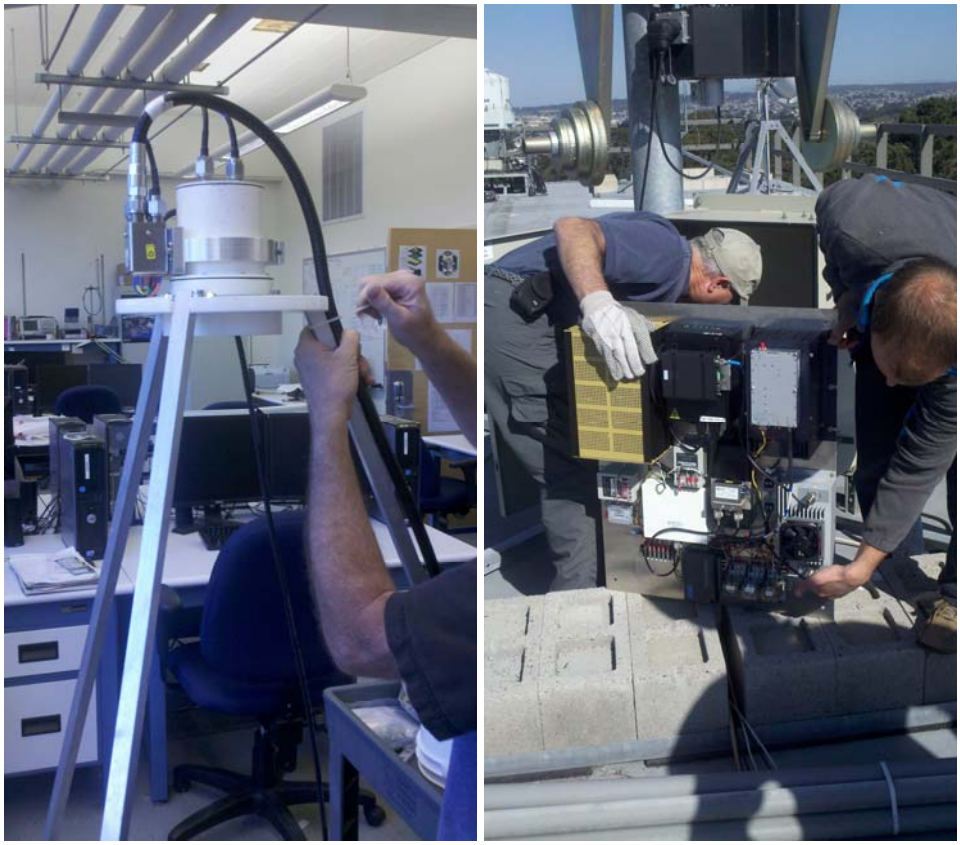

Figure 4. Dish feed assembly and electrical housing integration

## 4. Software

The 3-meter dish system's current status is monitored in the Satellite Ground Station Lab in Bullard Hall at NPS. The configuration of the lab is displayed in Figure 5. A simple graphical user interface (GUI) displays the dish azimuth, elevation, polarization and any warnings that may exist in the system. The GUI is one way users can control the dish system and monitor its status. The dish system can also be controlled through the Neptune software.

Figure 5. Satellite Ground Station Lab at NPS

## 5. Modification

Each MC3 node that incorporates a parabolic dish system will have to make individual decisions during mounting and construction to maximize the effectiveness of their antenna systems. In December 2013, physical modifications were made to the dish system at NPS to test whether or not the slew rate could be increased. The original configuration of the dish system included counterweights, shown in Figure 3, on the rear arm of the dish system.

M2 Antenna Systems provided 12 separate weights as part of the assembly kit in the following sizes: 15 lbs., 10.25 lbs., and 5.3 lbs. The purpose of these weights, totaling 122.2 lbs., is to counterbalance the load of the parabolic dish, dish feed, and cabling. The weight of the dish feed and cabling to be used by this antenna was unknown to M2 Antenna Systems because they were not purchased from its company. Consequently, extra weights were sent in the assembly kit to account for the unknown weight of those components. When all the counterweights are placed on the arm, the maximum slew rate the dish system can accomplish is 3.2 degrees per second. A faster slew rate would allow the dish system to minimize the amount of time lost when affected by its keyhole constraint, as discussed in Chapter II, Section C of this thesis.

At NPS, to test for a faster slew rate, the counterweights were removed in small increments. Then the dish system was commanded to move at increased slew rates between differing azimuths and elevations. As a result, the overall weight was lightened to approximately 80.5 lbs., creating a more optimally balanced dish system. The total slew rate has been increased slightly and is estimated to be 3.5 degrees per second. Further testing, discussed in Chapter IV, Section B, could be done to identify other ways to increase the slew rate.

## B. INITIAL POINTING CALIBRATION

Antenna calibration must be completed after the initial construction of the antenna and when regular maintenance or modifications are made. The calibration mentioned in this chapter refers to the pointing accuracy of the antenna. For the dish system to be pointed successfully, operators must ensure that the data displayed on the GUI accurately portrays the direction that the dish is pointed when stationary. Then, the pointing accuracy can be further refined by tracking an object in motion.

After the dish system was constructed, it was pointed toward an azimuth of true North and placed at zero degrees elevation, level with the ground plane. True North was estimated by entering the coordinates for the dish system into

Google Earth and drawing a straight line over the map towards true North. Then, an easily identifiable landmark along that straight line was chosen and the dish system was physically turned to point in its direction. Zero degrees azimuth and elevation establishes the zeroed state of the control motor. This zeroed state is verified through the GUI's display.

The accuracy of this simple calibration is tested by tracking the sun, an easily accessible celestial body. To track the sun, a Systems Tool Kit (STK) scenario is built to view its exact elevation and altitude with respect to the dish antenna. Then the dish system is commanded to execute a sun-tracking scenario. During the test, the GUI is referenced to monitor the dish's accuracy. In addition, the alignment of the dish antenna with the sun is visually verified. The shadow created by the dish system when it is pointed directly at the sun is symmetrical. If the dish system is not pointed correctly, the shadow will be skewed. If the antenna accurately tracks the sun's movement over a period of a few minutes then its pointing accuracy has successfully been calibrated.

## C. CONSTRAINTS

Unfortunately, the dish system has what is called a keyhole constraint. The keyhole prevents the dish system from tracking through north, an azimuth of zero or 360 degrees. Once the dish system nears this azimuth it must stop and unwind in the opposite direction of its approach to north. Also, if the dish system is tracking a spacecraft that will pass directly overhead at 90 degrees elevation, it will be forced to stop and rotate 180 degrees around its vertical axis to track the spacecraft's descent. This keyhole constraint costs valuable time during satellite passes. It can take up to two minutes, depending on the type of pass, for the dish system to rotate and acquire its target again. Chapter IV, Section B of this thesis discusses future work that could be done to eliminate the keyhole constraint at 90 degrees elevation.

Another limitation on this antenna is created from the surrounding mountainous terrain of the Monterey area. Unfortunately, the horizon, as viewed

from the top of Spanagel Hall, is blocked by mountains in several directions. Figure 6 portrays the elevation of the local terrain and estimated distance to two of the highest elevations. The dish system will have line-of-sight contact with a satellite rising from the west after it has crossed the mountains at approximately 3 degrees elevation. If a satellite approaches from the south it will have to rise to approximately 5 degrees elevation before the dish system will be line-of-sight and able to communicate. Luckily, to the northwest, the antenna is partially surrounded by the ocean. A satellite ascending from the ocean side of the antenna will have the longest opportunity to communicate with the dish system.

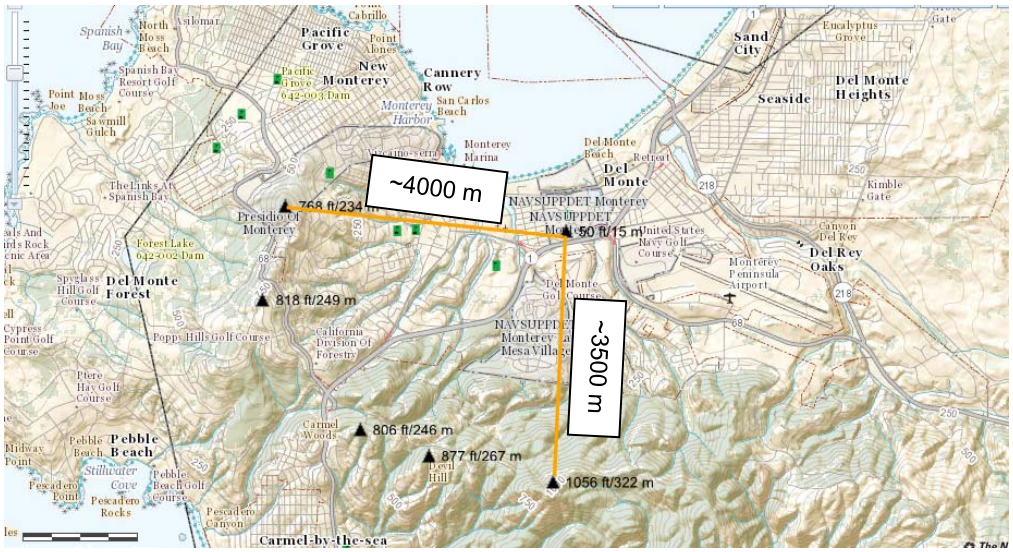


Figure 6. Spot elevations around the 3-meter dish system

The International Telecommunication Union (ITU) has placed restrictions on transmission from ground stations in space research service at frequencies bands above 1 gigahertz. The rule states,

> earth station antennas in the space research service (near Earth) shall not be employed for transmission at elevation angles of less than 5 degrees, and earth station antennas in the space research service (deep space) shall not be employed for transmission at elevation angles of less than 10 degrees, both angles being those measured from the horizontal plane to the direction of maximum radiation. [10]

Therefore, the terrain obstructions only affect the time the dish antenna has to receive data because transmissions from the dish have already been restricted at low elevation angles. Transmitting and receiving data from low elevation angles is often problematic because the signal passes through more of the atmosphere and can be affected more greatly by scintillation, atmospheric attenuation, and multipath errors. The spacecraft is the farthest distance from the antenna as it crosses over the horizon; therefore, the link with the ground station is at its weakest strength. On the other hand, if a link can be established, the time for receiving data is increased and the spacecraft will be at its slowest velocity with respect to the antenna slewing. All added communication time is valuable and increasingly so, if a satellite needs to send emergency information. Neptune software allows for this possibility because it starts listening for spacecraft transmissions at zero degrees elevation.

## D. LINK BUDGET

A sample link budget for the dish system was created by David Rigmaiden and is displayed in Table 2. This link budget reflects the performance of the 3-meter dish system when communicating with the NPS Solar Cell Array Tester (SCAT) CubeSat [9] from three different elevation angles. The SCAT CubeSat program is managed by the Space Systems Academic Group (SSAG) at NPS with the primary objective “to develop a space borne system that is capable of autonomously measuring the characteristics of several experimental solar cells to determine the rate of degradation” [8].

The sections of Table 2 that are highlighted in blue are input directly by the user of the spreadsheet. All other fields are calculated based on those inputs. When analyzing the bit energy-to-noise ratio, the highest link margin of 20.8 decibels, is established during a downlink from SCAT at an elevation angle of 90.0 degrees. The lowest link margin, 3.5 decibels, is established during an uplink to SCAT at an elevation angle of 10 degrees.

| Item | Units | Down Link | | | Up Link | | | | |
|---|---|---|---|---|---|---|---|---|---|
| Orbit Altitude | km | 560 | 560 | 560 | 560 | 560 | 560 | | |
| Spacecraft Elevation Angle | deg | 10 | 45 | 89.99 | 10 | 45 | 89.99 | | |
| Frequency | GHz | 2.44 | 2.44 | 2.44 | 2.44 | 2.44 | 2.44 | | |
| Wavelength | m | 0.123 | 0.123 | 0.123 | 0.123 | 0.123 | 0.123 | | |
| Propagation Path Length | km | 1839.27 | 762.30 | 560.00 | 1839.27 | 762.30 | 560.00 | SMAD p. 110-115 | |
| Space Loss - Ls | dB | -165.48 | -157.83 | -155.15 | -165.48 | -157.83 | -155.15 | | |
| System Noise Temperature - Ts | k | 585 | 585 | 585 | 585 | 585 | 585 | SMAD p. 556-558 | |
| Bit Error Rate | | 1.00E-05 | 1.00E-05 | 1.00E-05 | 1.00E-05 | 1.00E-05 | 1.00E-05 | | |
| Required Eb/No for BER 10-5 | dB | 13.5 | 13.5 | 13.5 | 13.5 | 13.5 | 13.5 | SMAD p. 562 | |
| Data Rate - Rb | kbps | 115.2 | 115.2 | 115.2 | 115.2 | 115.2 | 115.2 | | |
| Symbols Per Bit | | 1 | 1 | 1 | 1 | 1 | 1 | SMAD p. 559 | |
| Symbol Rate - Rs | kbps | 115.2 | 115.2 | 115.2 | 115.2 | 115.2 | 115.2 | | |
| ro | | 1.50 | 1.50 | 1.50 | 1.50 | 1.50 | 1.50 | | |
| Required C/No | dB | 64.11 | 64.11 | 64.11 | 64.11 | 64.11 | 64.11 | $E_b/N_o+10*\log(R_b)$ | |
| Bandwidth - BW | MHz | 0.288 | 0.288 | 0.288 | 0.288 | 0.288 | 0.288 | $(1+ro)*R_s$ | |
| Required C/N | dB | 9.52 | 9.52 | 9.52 | 9.52 | 9.52 | 9.52 | $C/N_o-10*\log(BW)$ | |
| Receiver Bandwidth - B | MHz | 0.4 | 0.4 | 0.4 | 0.4 | 0.4 | 0.4 | | |
| GND Antenna Diameter | m | 3.04 | 3.04 | 3.04 | 3.04 | 3.04 | 3.04 | | |
| GND Antenna Feed Efficiency | % | 55 | 55 | 55 | 55 | 55 | 55 | | |
| GND Antenna Half Power Beamw | deg | 2.83 | 2.83 | 2.83 | 2.83 | 2.83 | 2.83 | SMAD p. 571 | |
| GND Antenna Pointing Error | deg | 2.0 | 2.0 | 2.0 | 2.0 | 2.0 | 2.0 | | |
| GND Antenna Pointing Error Loss | dB | -7.65 | -7.65 | -7.65 | -7.65 | -7.65 | -7.65 | | |
| GND Antenna Gain - G | dBi | 37.81 | 37.81 | 37.81 | 37.81 | 37.81 | 37.81 | | |
| S/C Antenna Diameter | m | 0.0392 | 0.0392 | 0.0392 | 0.0392 | 0.0392 | 0.0392 | | |
| S/C Antenna Feed Efficiency | % | 90 | 90 | 90 | 90 | 90 | 90 | | |
| S/C Antenna Half Power Beamwi | deg | 360.00 | 360.00 | 360.00 | 360.00 | 360.00 | 360.00 | SMAD p. 571 | |
| S/C Antenna Pointing Error | deg | 0.0 | 0.0 | 0.0 | 0.0 | 0.0 | 0.0 | | |
| S/C Antenna Pointing Error Loss | dB | 0.00 | 0.00 | 0.00 | 0.00 | 0.00 | 0.00 | | |
| S/C Antenna Gain - G | dBi | 0.01 | 0.01 | 0.01 | 0.01 | 0.01 | 0.01 | | |
| Transmitter Power | Watts | 1 | 1 | 1 | 10 | 10 | 10 | | |
| Transmitter Power - P | dBW | 0.00 | 0.00 | 0.00 | 10.00 | 10.00 | 10.00 | | |
| Transmitter Line Loss - $L_l$ | dB | -0.5 | -0.5 | -0.5 | -1 | -1 | -1 | | |
| Transmitter Feed Loss - $L_a$ | dB | -0.46 | -0.46 | -0.46 | -2.60 | -2.60 | -2.60 | | |
| Transmitter EIRP | dBW | -0.94 | -0.94 | -0.94 | 44.21 | 44.21 | 44.21 | $EIRP=P+L_l+G_a+L_a$ | |
| Transmission Path Losses - $L_a$ | dB | -0.50 | -0.50 | -0.50 | -0.50 | -0.50 | -0.50 | | |
| Receiver Polarization Loss - L | dB | -3 | -3 | -3 | -3 | -3 | -3 | | |
| Receiver Line Loss - $L_a$ | dB | -1 | -1 | -1 | -0.5 | -0.5 | -0.5 | | |
| Receiver Feed Loss - $L_a$ | dB | -2.60 | -2.60 | -2.60 | -0.46 | -0.46 | -0.46 | | |
| Receiver LNA Gain | dB | 17.00 | 17.00 | 17.00 | 0.00 | 0.00 | 0.00 | | |
| Received Carrier Power - C | dBW | -126.37 | -118.72 | -116.04 | -133.37 | -125.72 | -123.04 | $C=EIRP+L_s+L_a+G$ | |
| Total Received Noise Power - | dB | -144.91 | -144.91 | -144.91 | -144.91 | -144.91 | -144.91 | $N=k*T_s*B$ | k=1.38E-23 |
| Received Carrier To Noise Ratio | dB | 18.54 | 26.19 | 28.87 | 11.54 | 19.19 | 21.87 | SMAD p. 550-556 | |
| Received Energy Per Bit - $E_b$ | dB | -176.98 | -169.33 | -166.65 | -183.98 | -176.33 | -173.65 | $E_b=C/R_s$ | |
| Received Noise Spectral Density | dB | -200.93 | -200.93 | -200.93 | -200.93 | -200.93 | -200.93 | $N_o=k*T_s$ | |
| Calculated Eb/No | dB | 23.95 | 31.60 | 34.28 | 16.95 | 24.60 | 27.28 | | |

Table 2. Sample link budget for S-band dish system and SCAT, from [9]

This link budget provides a basis for predicting MHX-2400 transceiver performance in the local hilltop testing discussed in Chapter III, Section A and the HAB test discussed in Chapter III, Section B.

## E. SUMMARY

This chapter addresses the careful installation and calibration of the 3-meter dish assembly by SmallSat personnel. It also documents the physical modifications that were made to the antenna system to allow for a higher slew rate. The keyhole constraint and elevation of local terrain were identified as factors that limit operations of the dish. With installation, calibration and the identification of limitations complete, the capabilities of the dish system could be tested. Chapter III discusses four experiments intended to test the dish system's ability to accurately point at and track a moving target, then create a link and receive data.

THIS PAGE INTENTIONALLY LEFT BLANK

# III. MC3 3-METER DISH CAPABILITIES TESTING

The Space Systems Academic Group at NPS is responsible for overseeing experimental development, testing, and mission operations for the MC3 ground station network [11]. Upgrading the MC3 network by implementing the 3-meter dish system will allow more robust operations for spacecraft utilizing S-band frequencies, such as NPS-SCAT and upcoming Colony CubeSats. Modifying the parabolic dish system with a UHF feed antenna could allow further benefits for the MC3 network through its higher gain and greater pointing accuracy. Therefore, the capabilities of the dish system were tested from a variety of distances with differing levels of dynamic movement to verify the ability of the system to track a spacecraft, create a link and receive data via UHF and S-band frequencies. The first communications test involved a Microhard MHX-2400 wireless transceiver that was taken to hilltops in the vicinity of NPS. The next two tests involved high altitude balloons (HABs). The final test sequence involved the Space Communications and Navigation (SCaN) Testbed aboard the International Space Station (ISS).

## A. NEARBY HILLTOP TESTING

### 1. Purpose

Testing within the local area had a threefold purpose: to verify that the 3-meter dish system internal MHX-2400 hardware was installed properly, that the dish antenna could establish a link with another MHX-2400 transceiver and that data could be successfully received. This supports the goal of this thesis to identify the capabilities of the dish system.

### 2. Method

To accomplish these goals, the following steps were completed:

- Three hilltop locations with progressively longer distances from NPS were identified
- A mobile MHX-2400 radio system was set up in field locations

- Test messages of differing lengths were sent from the field locations to the dish antenna located at NPS
- Signal strengths were recorded

### 3. Test Locations

Test locations were chosen based on line-of-sight contact with the 3-meter dish and accessibility. The three locations chosen for testing were Jack's Peak, San Benancio Road near Mount Toro, and Fremont Peak. GoogleEarth was used to determine the azimuth and distance from the dish system to each location, which is displayed in Figure 7.

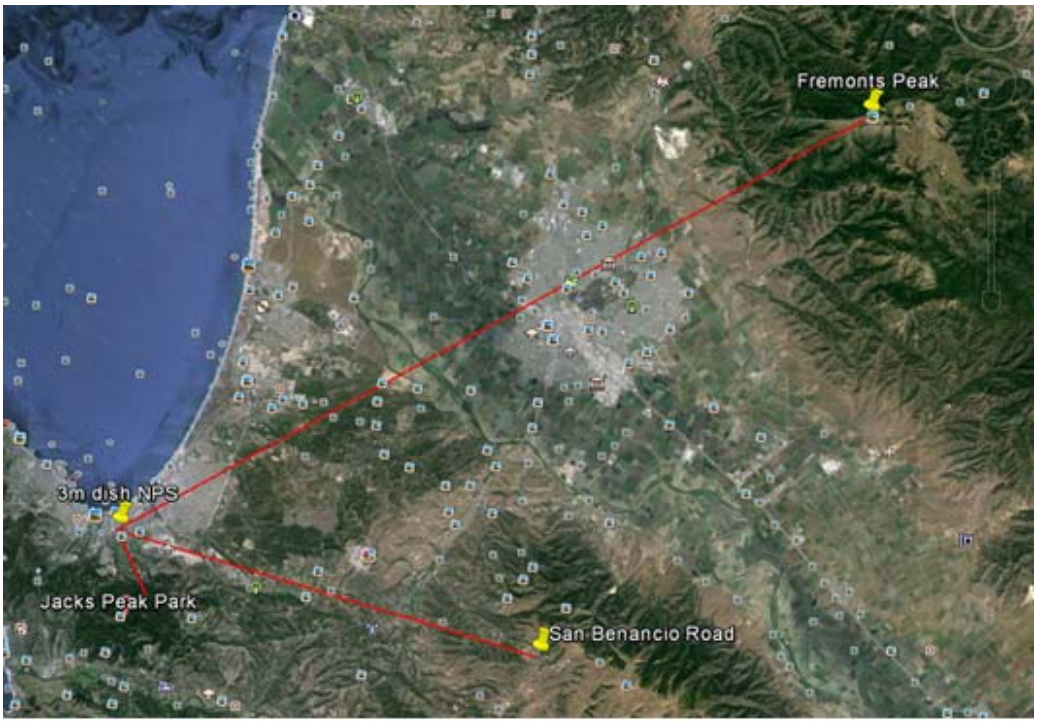


| Location | Heading | Distance |
|---|---|---|
| Jack's peak | 155 degrees | 1.97 miles |
| San Benancio Rd | 107 degrees | 12 miles |
| Fremont's peak | 61 degrees | 23.4 miles |

Figure 7. MHX radio testing locations

## 4. Equipment

The Microhard MHX-2400 is a frequency-hopping, spread-spectrum transceiver with an operating range from 2.4 to 2.4835 GHz [7]. One of these transceivers has been incorporated into the dish antenna electrical housing box. It was incorporated to support CubeSat missions, such as NPS-SCAT, which use an MHX-2400 as their primary communication radio [9]. The S-band dish system can shift operation between the GDP receiver and the MHX-2400 transceiver via a physical operational switch inside its electrical housing.

For this test, an MHX-2400 development kit, shown in Figure 8, was used to create a mobile radio system for field testing (Figure 9). The complete system consists of an MHX2400 development board, antenna, serial port cord, power cord, custom-made metal frame and laptop. SmallSat engineers created the metal frame to house the MHX-2400 for the purpose of stabilization and protection of the transceiver while in the field. The laptop used in the field test was equipped with Tera Term software, a terminal emulator program.

Figure 8. MHX-2400 development kit, from [6]

Figure 9. Mobile MHX-2400 radio system used for field testing

## 5. Hilltop Test Procedure

First, the author drove to one of the predetermined locations, in Figure 7, and set up the MHX-2400 radio system. Then the author positioned the antenna to have line-of-sight access to the 3-meter dish system. Next, a phone call between the author and a team member at the NPS SOC was made. Throughout the test, verbal confirmation of the digital messages sent and received was made.

Once a link was established, four separate test messages of differing lengths were transmitted to the dish antenna. They are displayed in Appendix A. The test messages were chosen so errors could be easily identified. During the tests, the received signal strength indicator (RSSI) value was recorded. The RSSI represents "the average signal strength in dBm over the previous four hop intervals" [7]. The MHX-2400 manual suggests a signal strength above -95 decibel-milliwatts (dBm) be maintained for effective communication [7]. The integrity of the messages sent and the signal strength determined the success of each test.

## 6. Results

Table 3 displays the results of the testing done at Jack's Peak, San Benancio Road, and Fremont Peak. Table 3 displays the name of each test message that was sent, the azimuth and elevation angle of the 3-meter dish and RSSI values when measured. RSSI values were measured once at Jack's Peak, twice at San Benancio Road and eight times at Fremont Peak. Table 3 also displays the number of characters missing in the test messages received by the 3-meter dish. The number of characters including spaces that were in each of the original test messages are:

- Test 1: 44 characters
- Test 2: 150 characters
- Test 3: 1,449 characters
- Test 4: 7,670 characters

| MHX-2400 Testing | | | | | | | | |
|---|---|---|---|---|---|---|---|---|
| Date | Location (Distance from NPS in miles) | Power Output of MHX in Field Location | 3-Meter Dish Azimuth (deg) | 3-Meter Dish Elevation (deg) | Name of Test Message Sent to Dish | RSSI Value (dBm) | # of Missing Characters in Received Message | Estimated Link Margin (dB) |
| 25-Oct-13 | Jack's Peak (1.97) | 10 mW | 155 | 0 | Test 2 | | 0 | |
| | | 10 mW | 155 | 0 | Test 3 | | 0 | |
| | | 10 mW | 155 | 0 | Test 4 | | 0 | |
| | | 10 mW | 155 | 0 | Test 2 | | 0 | |
| | | 10 mW | 155 | 0 | Test 3 | | 0 | |
| | | 10 mW | 155 | 0 | Test 4 | -58 | 0 | 59.7 |
| 29-Oct-13 | San Benancio Rd (12) | 50 mW | 107 | 3 | Test 1 | | 0 | |
| | | 50 mW | 107 | 3 | Test 2 | | 0 | |
| | | 50 mW | 107 | 3 | Test 3 | | 225 | |
| | | 50 mW | 107 | 3 | Test 4 | | 524 | |
| | | 50 mW | 107 | 3 | Test 4 | -78 | 2099 | 39.7 |
| | | 10 mW | 106 | 3 | Test 2 | | 0 | |
| | | 10 mW | 106 | 3 | Test 3 | | 0 | |
| | | 10 mW | 106 | 3 | Test 4 | | 0 | |
| | | 10 mW | 106 | 3 | Test 2 | | 0 | |
| | | 10 mW | 106 | 3 | Test 3 | | 0 | |
| | | 10 mW | 106 | 3 | Test 4 | -59 | 0 | 58.7 |
| 5-Nov-13 | Fremont's Peak (23.4) | 1 W | 61 | 3 | Test 1 | | 0 | |
| | | 1 W | 61 | 3 | Test 2 | | 0 | |
| | | 1 W | 61 | 3 | Test 3 | | 0 | |
| | | 1 W | 61 | 3 | Test 4 | | 0 | |
| | | 1 W | 51 | 3 | N/A | -84 | N/A | 33.7 |
| | | 1 W | 71 | 3 | N/A | -95 | N/A | 22.7 |
| | | 1 W | 58 | 3 | N/A | -59 | N/A | 58.7 |
| | | 1 W | 61 | 5 | Test 1 | -83 | 0 | 34.7 |
| | | 1 W | 59.5 | 3 | N/A | -56 | N/A | 61.7 |
| | | 1 W | 61 | 1 | Test 1 | -83 | 0 | 34.7 |
| | | 1 W | 55 | 1 | Test 1 | -66 | 0 | 51.7 |
| | | 1 W | 55 | 1 | Test 3 | -62 | 0 | 55.7 |

Table 3. MHX-2400 testing results from nearby hilltops

Additionally, the author implemented the following equation from *Space Mission Engineering: The New SMAD* in Table 4 to evaluate and estimate the link margin [20].

$$\text{Received } \frac{E_b}{N_o} = \frac{P_r \sin^2(\beta)}{N_o R}$$

The results of the estimated link margin are recorded in the last column of Table 3. RSSI values were entered into Table 4 as the total received power. Then an average temperature of 60º Fahrenheit and a required bit energy-to-noise ratio (Eb/No) of 13.5 decibels were used to complete the calculation.

| Estimated Link Margin for MHX-2400 Downlink | | | |
|---|---|---|---|
| Information Bit Rate | 9600.0 | bps | |
| Information Bit Rate ( R ) | 39.82 | | = 10*LOG(Information Bit Rate) |
| Data To Total Power | 0.0 | dB | |
| Total Received Power (Pr) | -58.0 | dBm | |
| Boltzmann's Constant (k) | 1.38065E-23 | J/K | |
| Temperature in Fahrenheit (Temp) | 60.0 | F | |
| Temperature in Kelvin | 288.7 | K | = (Temp-32) * (5/9) + 273.15 |
| System Noise Density | 3.98601E-21 | J | = k * Temperaure in Kelvin |
| System Noise Density (No) | -174.0 | dBm/Hz | = 10 * LOG( 1000 * System Noise Density) |
| Received Eb/No | 76.2 | dB | = Pr + (Data To Total Power) - No - R |
| Required Eb/No | 13.5 | dB | |
| Receiver System Loss | -3 | dB | |
| **Link Margin** | 59.7 | dB | = Received Eb/No - Required Eb/No + Receiver System Loss |

Table 4. Estimated Link Margin Calculator

No errors were received in the transmission from Jack's Peak, the location closest to NPS. The average signal strength of messages received by the 3-meter dish was -58 dBm. This signal strength is well above the minimum signal strength of -95 dBm suggested by the MHX-2400 manual to maintain communications. This is also reflected in the link margin calculation of 59.7 decibels.

There were several errors received in the initial testing from San Benancio Road. Troubleshooting the hardware connections of the MHX-2400 in the field revealed that the antenna of the MHX-2400 needed to be tightened. Then the power of the MHX-2400 in the field was reduced to 10 milliwatts and the azimuth

of the 3-meter dish was adjusted 1 degree. After these changes occurred, all messages sent from the field MHX-2400 were received with no error. The highest RSSI value was -59 dBm.

From the Fremont Peak location, there were no errors received during testing. At this location the dish was turned off of its original azimuth of 61 degrees to test the limits of the dish assembly's abilities. Each time the dish was moved to a new azimuth, the azimuth was recorded along with the new RSSI value. Then MC3 personnel typed a message through Tera Term consisting of the new azimuth for the author to view in the field. Full test messages were not necessary to be sent after each heading change because RSSI values verified the strength of the signal and performance of the dish assembly. The greatest deviation from the center azimuth was 11.5 degrees. At that azimuth, the signal strength was -95 dBm, which is the lowest recommended strength. The link margin at that azimuth was estimated to be 22.7 decibels.

The testing at Fremont Peak also revealed that 59.5 degrees azimuth (not 61 degrees) was the optimal azimuth for transmissions. The arc length between these two azimuths is approximately 0.6 miles. Originally, it was thought that this 1.5 degree difference was created by testing from a location that was not exactly at the top of Fremont Peak. The azimuth from the dish assembly to Fremont Peak was measured using GoogleEarth; it is 61.3 degrees. The actual test location was a dirt road slightly offset from the peak; it is 61.4 degrees from the dish assembly. Therefore, this could not be the reason for the difference between the optimal heading and actual azimuth to the test location. The difference in azimuths could be an indicator that dish's pointing accuracy needs to be recalibrated. The full reason for the 1.5 degree difference is not known and is beyond the scope of this thesis. Future work could be done to further understand this difference in azimuth.

Overall, the success of these three tests verified the 3-meter dish system internal MHX-2400 hardware was installed properly, the dish antenna could establish a link with another MHX-2400 transceiver and data could be

successfully received. This supports the goal of this thesis to identify the capabilities of the dish system.

## B. HIGH ALTITUDE BALLOON TEST S-BAND

High altitude balloon (HAB) tests are used by many space-oriented companies and universities for testing communications equipment [11]. These tests are valuable to NPS because of their low cost, relatively short execution time and extensive educational value to NPS students and SmallSat lab interns. The tests have been used to validate MC3 ground station operation and assess the capabilities of radios that will be incorporated into university CubeSats.

### 1. Project Stratosphere

*Project Stratosphere* is a HAB test currently being designed and executed by interns with support of SmallSat engineers. The project started in August 2013 and is projected to be complete by July 2014. The overall goal of the test is to "validate the capability of a cross-country HAB flight" [13]. During the execution of this HAB flight, the MC3 ground stations located at NPS, USU and AFIT may be utilized for communications.

In December 2013, *Project Stratosphere* conducted a local communications HAB flight in preparation for the cross-country flight. A decision on the primary radio to use in the payload had not been made. There were two radio possibilities for the cross-country flight. One of the options was the Microhard MHX-2400 transceiver, which operates in S-band frequencies. The other prospect was the Astro devices (AstroDev) Kevin Brown Radio (KBR), which operates in UHF. The MHX-2400 radio was chosen to be fielded in this particular local HAB flight.

### 2. Purpose of the S-band HAB Flight

The primary purpose of this HAB test was to provide operational data to aid decision-makers in choosing a radio for use in the *Project Stratosphere*

payload. The secondary purpose supports this thesis by validating the MC3 dish antenna's ability to point accurately, create a link and receive data via MHX-2400 S-band frequencies.

## 3. HAB Communications Payload

The payload being carried by the HAB consists of the following components:

- Fuselage (Cardboard Rocket Body)
- MHX-2400 Transceiver
- Beagle-Bone Black (BBB) Single Board Computer
- Circuit board with radio mount
- GPS (GT-320FW) receivers (x2)
- Automatic Packet Reporting System (APRS) with whip antenna
- Satellite Position and Tracking (SPOT)
- Temperature/Humidity Data Logger (RHTemp101A)
- Patch antenna
- Battery packs

The payload was constructed and tested in the SmallSat lab. SmallSat engineers and interns worked together to design the fuselage of the payload from a cardboard rocket body. They integrated each of the components above and designed software using Python code to allow the components to communicate with one another through the BBB. Figure 10 shows the payload before it was fully integrated, this configuration allowed for system testing outside the SmallSat lab.

Figure 10. S-band HAB payload testing at NPS

### *a. BBB Single Board Computer*

The BBB, Figure 11, is a single board computer. It has four universal asynchronous receiver/transmitters (UARTs). For this HAB experiment, two components were connected to the UARTs: one GPS receiver and the MHX-2400. Python code was developed by interns with support from SmallSat Lab personnel to control all BBB functions.

Figure 11. BBB

### *b. GPS Receivers*

Two GPS receivers, Figure 12, were incorporated into the HAB payload. One receiver provided position data to the APRS. The other receiver provided position data to the BBB. The BBB formatted the GPS data into National Marine Electronics Association (NMEA) packets and sent them to the MHX-2400. Then, those packets were transmitted, via the patch antenna.

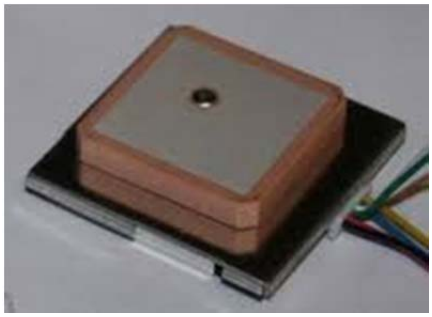

Figure 12. GPS receiver

### *c. Automatic Packet Reporting System*

The Automatic Packet Reporting System (APRS) transmitter has its own power source and antenna. One APRS transmitter was incorporated into the HAB payload. The APRS was used to transmit location data that was uploaded through the APRS network to the following website, http://aprs.fi [14]. The website was accessed during the balloon's flight by team members in chase vehicles for tracking and payload recovery purposes.

### *d. SPOT Tracker*

Several SPOT trackers (Figure 13) were used during HAB flight operations. One SPOT tracker was placed in each chase vehicle and one was incorporated into the HAB payload. The SPOT tracker is a standalone device with its own power source and antenna. The SPOT tracker periodically

transmitted its location, which was viewed during flight operations on the following website, https://login.findmespot.com/spot-main-web/auth/login.html, for tracking and recovery purposes [15].

Figure 13. SPOT tracker

## 4. Location of Balloon Release

The geography of local terrain, safety precautions, flight path prediction software and historical HAB flight examples were used to determine the location for balloon launch and recovery. Highly populated areas, airports, power lines and other obstructions were avoided to ensure safety of the local populace and successful operations.

The following free online applications were used for flight prediction:

- http://astra-planner.soton.ac.uk/
- http://predict.habhub.org/

The prediction software revealed that the flight path of the balloon would follow a south to southeast route. This is an ideal situation for a balloon released in the Central Valley of California because during the flight the payload will not cross over mountainous terrain. Therefore, Chowchilla, California, was chosen as the primary location for launch. Figure 14 displays the results from the prediction software run on December 19, 2013 for the launch date of December 21, 2013.

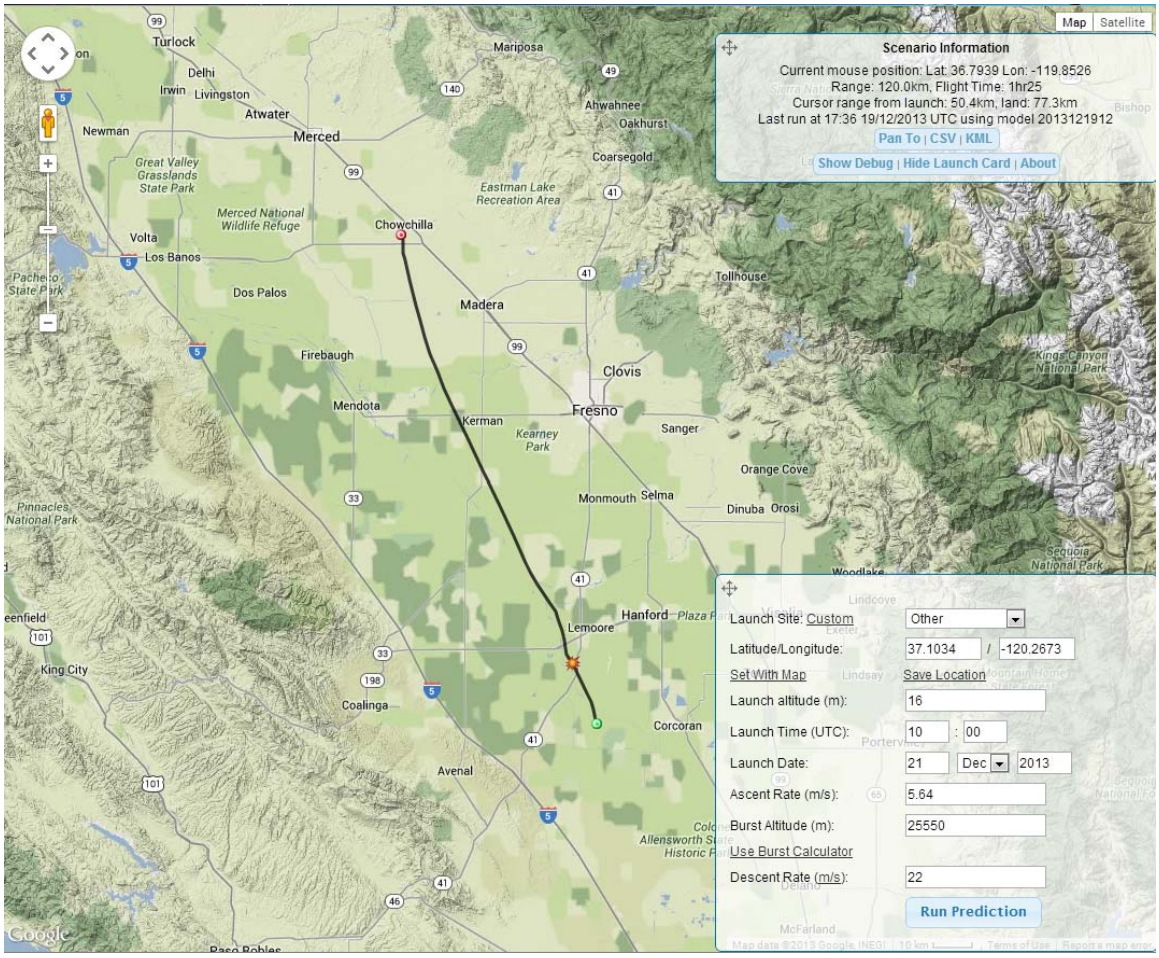


Figure 14. HAB flight prediction for December 21, 2013

## 5. Procedure for HAB Communications

On the morning of the launch day, end-to-end testing of the payload was conducted in the SmallSat lab to ensure all components were working properly. The entire system was checked again upon arrival at the launch site. To accomplish this, a mobile MHX-2400 radio system (discussed in Chapter III Section A of this report) was set up by the author. Then Tera Term software was run to monitor transmissions being sent by the balloon's MHX-2400 radio. Once transmissions of accurate GPS data were received, the HAB crew concluded that the GPS was receiving accurate data, the BBB was processing and sending data correctly, and the MHX-2400 was successfully transmitting through the patch antenna.

After positive communication was verified on the ground, the balloon was inflated (Figure 15) and subsequently, walked into a nearby field and launched (Figure 16). MC3 personnel stationed at the SOC at NPS were contacted and informed of the balloon's release time. During the initial stages of the flight, it was anticipated that the transmissions from the balloon's MHX-2400 would be blocked from the 3-meter dish at NPS by a mountain range. Therefore, the author used the mobile MHX-2400 radio system at the launch site to monitor the initial transmissions from the balloon while the MC3 personnel monitored the APRS and SPOT tracker data being transmitted by the balloon. Once the HAB had risen above 795 meters, the 3-meter dish began receiving data and all information was recorded.

Data was transmitted through three components on the HAB payload: the MHX-2400, APRS, and the SPOT tracker. Communications with the MC3 dish system were established through the balloon's MHX-2400 via its patch antenna. The information sent by the MHX-2400 was GPS data formatted by the BBB into NMEA packets. Location data was also transmitted from the APRS and SPOT tracker to their associated networks and displayed through their respective websites. APRS and SPOT tracker data were utilized in a supporting role to track the payload throughout its flight and aid in its recovery.

Figure 15. S-band HAB inflation

Figure 16. S-band HAB release

## 6. Results

Table 5 displays some of the data points recorded during the HAB flight. The first and last row of Table 5 correspond to the first and last time data was received by the dish assembly. The first column records the time a message was received by the 3-meter dish antenna in coordinated universal time (UTC). The second column is the GPS time stamp in the data received in UTC. The third column displays the ground distance between the HAB and the dish assembly. The fourth and fifth column reveal the GPS altitude in the message received and the RSSI value. The first messages received by the 3-meter dish antenna from 20:09 and 20:13 UTC on December 21, 2013 are recorded in Appendix B.

| Time Message Received by 3-meter dish hr:min (UTC) | GPS Time in Message hr:min (UTC) | Ground Distance Between 3-Meter Dish and HAB (km) | GPS Altitude Transmitted from HAB (m) | RSSI Value (dBm) |
|---|---|---|---|---|
| 20:09 | 19:55 | 154.6 | 94 | -102 |
| 20:12 | 19:58 | 154.6 | 944 | -102 |
| 20:13 | 19:59 | 154.6 | 1,255 | -102 |
| 20:14 | 20:00 | 154.6 | 1,578 | -103 |
| 20:16 | 20:02 | 154.4 | 2,186 | -106 |
| 20:19 | 20:05 | 153.4 | 3,054 | -97 |
| 20:20 | 20:06 | 153.3 | 3,589 | -83 |
| 20:21 | 20:07 | 153.2 | 3,920 | -79 |
| 20:23 | 20:09 | 153.1 | 4,253 | -79 |
| 20:27 | 20:13 | 153.2 | 5,486 | -77 |
| 20:32 | 20:17 | 153.7 | 6,719 | -80 |
| 20:40 | 20:25 | 157.1 | 8,723 | -83 |
| 20:50 | 20:36 | 171.5 | 11,728 | -80 |
| 20:56 | 20:42 | 180.7 | 13,316 | -90 |
| 20:58 | 20:44 | 183.0 | 13,744 | -103 |
| 21:03 | 20:49 | 190.5 | 15,117 | -78 |
| 21:11 | 20:58 | 198.5 | 17,546 | -87 |
| 21:22 | 21:08 | 202.8 | 20,703 | -83 |
| 21:27 | 21:11 | 203.9 | 21,826 | -78 |
| 21:32 | 21:16 | 204.1 | 23,335 | -106 |
| 21:37 | 21:23 | 204.3 | 25,317 | -84 |
| 21:41 | 21:28 | 206.2 | 27,345 | -86 |
| 21:52 | 21:38 | 210.5 | 31,033 | -88 |
| 21:53 | 21:39 | 210.7 | 31,210 | -99 |

Table 5. RSSI values for MHX-2400 HAB flight

There is a 14-minute difference between time data was received by the 3-meter dish and the GPS time stamp within the received packets. This difference is most likely because of Python coding used by the BBB to handle the incoming

GPS data and the outgoing MHX radio messages. The BBB apparently buffered the incoming information until a link with the 3-meter dish could be established. The link was expected to occur as the HAB climbed above 795 meters. The data reveals that at a GPS time of 20:09 UTC, when the first packet of information was received by the 3-meter dish, the HAB was at an altitude of 4,253 meters (13,953 feet). Once a link was established with the dish assembly, the BBB began to release packets of information in the order they were received.

The MHX-2400 manual states that "the minimum strength for communication is roughly -105 dBm" [7]. During the majority of the HAB operations, the RSSI values remained above this. The dish assembly maintained the link throughout the HAB's climb to a culminating altitude of 31.8 kilometers (104,491 feet) at 21:41 UTC. The last data set received by the 3-meter dish was at 21:53 when the HAB had begun its decent and its actual altitude was 10,222 meters (33,537 feet). It is unknown why transmissions ceased at that altitude. Throughout the flight, MC3 personnel used APRS data and MHX-2400 received messages to command the dish assembly to point in the direction of the HAB. The success of this test validated the ability of the MC3 dish antenna to point accurately, create a link with a radio at near orbital distances, and receive data via S-band frequencies.

## C. SCAN TESTBED

The Space Communications and Navigation (SCaN) Testbed Project is run by the National Aeronautics and Space Administration (NASA) Glenn Research Center. It was developed to

> provide NASA, industry, other Government agencies, and academic partners the opportunity to develop and field communications, navigation, and networking technologies in the laboratory and space environment based on reconfigurable, software-defined radio (SDR) platforms and the Space Telecommunications Radio System (STRS) Architecture. [12]

The SCaN Testbed Project incorporates a flight segment aboard the ISS and a ground station segment located in White Sands, New Mexico and Wallops Island, Virginia [12]. The ground segment also includes supporting infrastructure such as the SCaN Testbed Control Center, the Huntsville Operations Center, and the NASA Integrated Service Network. For this test, the normal SCaN ground stations were replaced by the MC3 ground station located at NPS. Figure 17 displays an overview of SCaN operations. The purpose of this test was to examine the MC3 dish system's ability to track a live satellite and maintain a link.

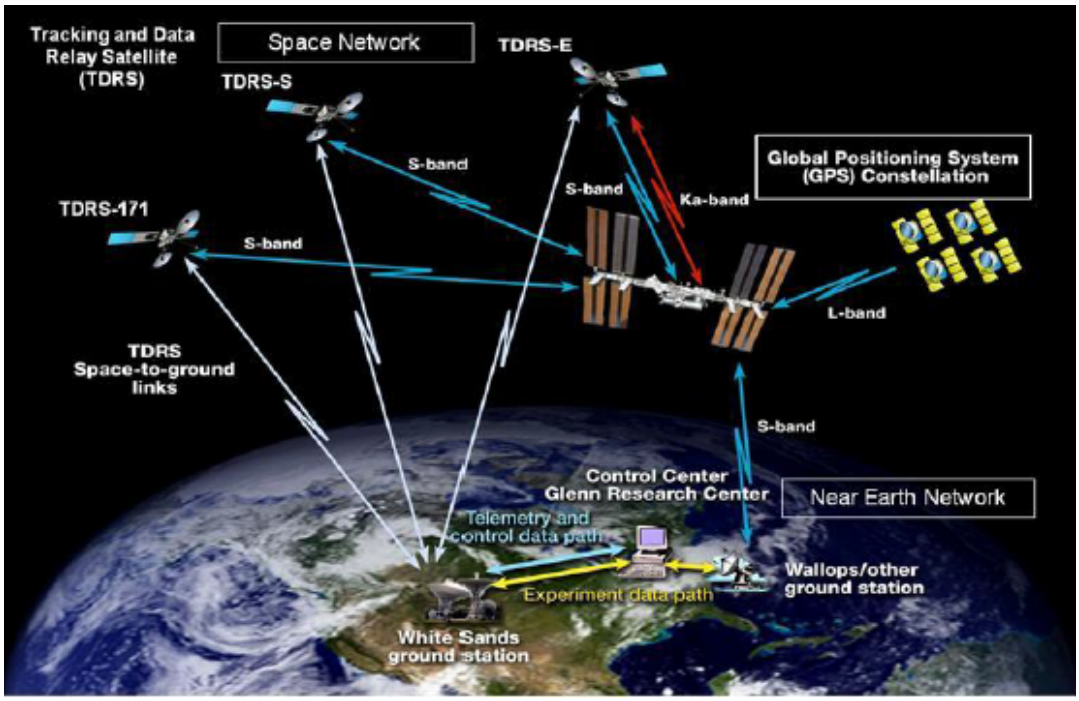


Figure 17. SCaN Testbed system overview, from [12]

### 1. SDRs aboard the ISS

The SCaN Testbed consists of three individual SDRs provided by the Jet Propulsion Laboratory (JPL), the Harris Corporation, and General Dynamics. These versatile radios enable the SCaN Testbed to communicate directly with ground stations via S-band frequencies or through the Tracking and Data Relay Satellite System (TDRSS) via S-band and Ka-band frequencies [12]. They also

receive L-band data from the Global Positioning System (GPS). Figure 18 is taken from the *SCaN Testbed Project* report; it graphically displays the SCaN Testbed in the stowed configuration.

The SCaN SDR employed for this experiment was the one provided by JPL. It is capable of transmitting in the 2.025–2.120 GHz frequency range and receiving in the 2.2–2.3 GHz frequency range [12]. Also, it has a 10 watt power amplifier that is estimated to provide 7.5 watts of power after losses [12].

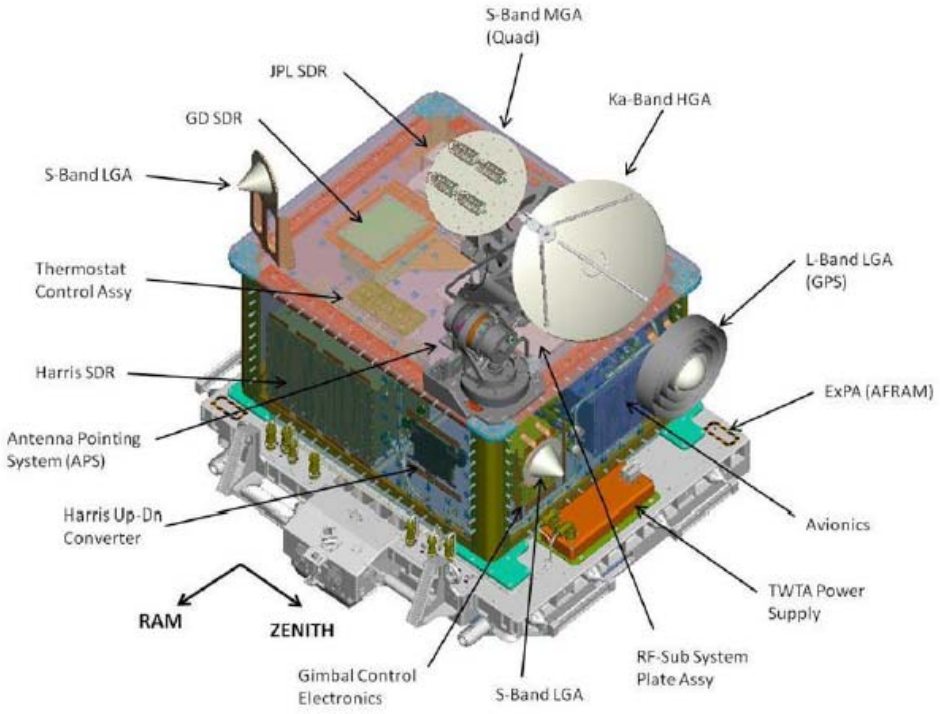


Figure 18. SCaN Testbed major components viewed from ram/zenith angle (stowed position shown), from [12]

### 2. Testing Proposal

To validate 3-meter dish operation, NPS proposed that the following two tests be conducted:

- The SCaN Testbed will transmit a binary phase shift keying (BPSK) waveform at 2106.40625 MHz (multiple access/ S-band multiple access) or 2041.02708 (S-band single access), which will be

received by the NPS 3-meter dish. Signal strengths will be measured, thus validating pointing capabilities and receiver performance.

- The NPS dish will radiate a continuous wave (CW) signal to the SCaN Testbed at 2287.5 MHz (multiple access/ S-band multiple access) or 2216.5 MHz (S-band single access). Based on the signal strength readings seen on the SCaN payload, this test will verify the transmitting capabilities of the dish system.

### 3. Testing Equipment at NPS

For the purposes of this test, a spectrum analyzer and an ETTUS SDR [19] with an SBX 400-4400 MHz transceiver were utilized. Figure 19 and Figure 20 display the ETTUS SDR and its performance specification. Each of these devices was monitored during the ISS passes to access signal strength, persistence of signal shape, and Doppler shift.

Figure 19. ETTUS SDR, from [19]

| Spec | Typ. | Unit |
|---|---|---|
| **POWER** | | |
| DC Input | 6 | V |
| Current Consumption | 1.3 | A |
| w/ WBX Daughterboard | 2.3 | A |
| **CONVERSION PERFORMANCE AND CLOCKS** | | |
| ADC Sample Rate | 100 | MS/s |
| ADC Resolution | 14 | bits |
| ADC Wideband SFDR | 88 | dBc |
| DAC Sample Rate | 400 | MS/s |
| DAC Resolution | 16 | bits |
| DAC Wideband SFDR | 80 | dBc |
| Host Sample Rate (8b/16b) | 50/25 | MS/s |
| Frequency Accuracy | 2.5 | ppm |
| w/ GPSDO Reference | 0.01 | ppm |

| Spec | Typ. | Unit |
|---|---|---|
| **RF PERFORMANCE (W/ WBX)** | | |
| SSB/LO Suppression | 35/50 | dBc |
| Phase Noise (1.8 Ghz) | | |
| 10 kHz | -80 | dBc/Hz |
| 100 kHz | -100 | dBc/Hz |
| 1 MHz | -137 | dBc/Hz |
| Power Output | 15 | dBm |
| IIP3 | 0 | dBm |
| Receive Noise Figure | 5 | dB |
| **PHYSICAL** | | |
| Operating Temperature | 0 to 55° | C |
| Dimensions (l x w x h) | 22x16x5 | cm |
| Weight | 1.2 | kg |

* All specifications are subject to change without notice.

Figure 20. ETTUS specifications, from [19]

## 4. Procedure for SCaN Testbed Experiment

Unfortunately, the MC3 at NPS did not have permission to transmit from the 3-meter dish system before the scheduled passes for this test occurred. Therefore, during this experiment, the dish antenna was limited to receive-only operations with the SCaN Testbed. To conduct this test, a schedule of contacts between the ISS and the 3-meter dish system was created. Contacts were chosen if they were daylight passes with acceptable elevation angles and durations.

During the scheduled times, personnel at the MC3 SOC stayed in contact with the SCaN Testbed operations center via phone. The MC3 personnel commanded the 3-meter dish system to track the ISS through Neptune software, which propagated a scenario using the ephemeris of the ISS. Then the spectrum analyzer and ETTUS SDR displays were referenced by the author and MC3 personnel and the signal strength recorded.

## 5. Results

Table 6 displays the schedule for the tests and expected highest elevation angles of the ISS with respect to the dish assembly. An updated timeline was emailed from the SCaN Testbed engineers hours before each contact to ensure MC3 personnel had the most accurate information. The remarks column in Table

6 was used to indicate whether or not each pass was recorded successfully by the ETTUS. The signal was recorded throughout the entire pass of three separate scheduled events. The final two columns display the highest amplitude of the received signal and the fast Fourier transform (FFT) value.

| Date | Start Time (PST) | | | Estimated Highest Elevation Angle (deg) | | | End Time (PST) | | | Remarks | Amplitude of Received Signal (dB) | FFT (dB) |
|---|---|---|---|---|---|---|---|---|---|---|---|---|
| Date | Time | Alt. | Az. | Time | Alt. | Az. | Time | Alt. | Az. | | | |
| 16-Jan | 10:25:44 | 10° | NW | 10:29:03 | 68° | NE | 10:32:22 | 10° | ESE | Preamp problems | N/A | N/A |
| 16-Jan | 12:05:11 | 10° | WSW | 12:05:20 | 10° | SW | 12:05:29 | 10° | SW | Preamp problems | N/A | N/A |
| | | | | | | | | | | | | |
| 17-Jan | 9:37:04 | 10° | NW | 9:40:12 | 37° | NE | 9:43:20 | 10° | ESE | Preamp problems | N/A | N/A |
| 17-Jan | 11:14:17 | 10° | W | 11:16:43 | 19° | SW | 11:19:09 | 10° | S | Preamp problems | N/A | N/A |
| | | | | | | | | | | | | |
| 21-Jan | 7:58:12 | 10° | NNW | 8:01:15 | 33° | NE | 8:04:18 | 10° | E | Setup problem | N/A | N/A |
| | | | | | | | | | | | | |
| 22-Jan | 7:10:33 | 10° | NNW | 7:12:10 | 21° | NNE | 7:14:48 | 10° | E | Signal Recorded | -85.46 | -92.75 |
| 22-Jan | 8:47:50 | 10° | WNW | 8:48:59 | 40° | SW | 8:52:07 | 10° | SSE | Signal Recorded | -79.39 | -83.35 |
| | | | | | | | | | | | | |
| 23-Jan | 7:59:00 | 10° | NW | 7:58:00 | 68° | NE | 8:00:35 | 10° | ESE | Signal Received/ Recording problem | N/A | N/A |
| 23-Jan | 9:37:20 | 10° | NW | 9:34:20 | 19° | SW | 9:35:20 | 10° | S | Signal Received/ Recording Problem | N/A | N/A |
| | | | | | | | | | | | | |
| 24-Jan | 7:10:40 | 10° | NW | 7:09:00 | 33° | NE | 7:12:00 | 10° | E | Signal Recorded | -85.13 | -96.81 |

Table 6. Schedule of passes for SCaN Testbed experiments

The SCaN Testbed experiments did not occur on the first two scheduled days because a problem was discovered with the preamplifier in the 3-meter dish assembly. Testing did not occur on the third scheduled day because a problem occurred while setting up the ETTUS and spectrum analyzer. After the problems were corrected by SmallSat engineers, normal testing began on January 22, 2014. On the final three days of testing a signal was successfully received by the ETTUS. Unfortunately, an unknown error in the recording or saving process occurred on January 23, 2014, which prevented the signal from being played back following testing on that day. The author, along with SmallSat personnel, identified the transmissions from the SCaN Testbed through the frequency, signal strength and persistence of the signal shape. Figures 21–23 show the FFT plot of the two passes on January 22, 2014 and one pass on January 24, 2014.

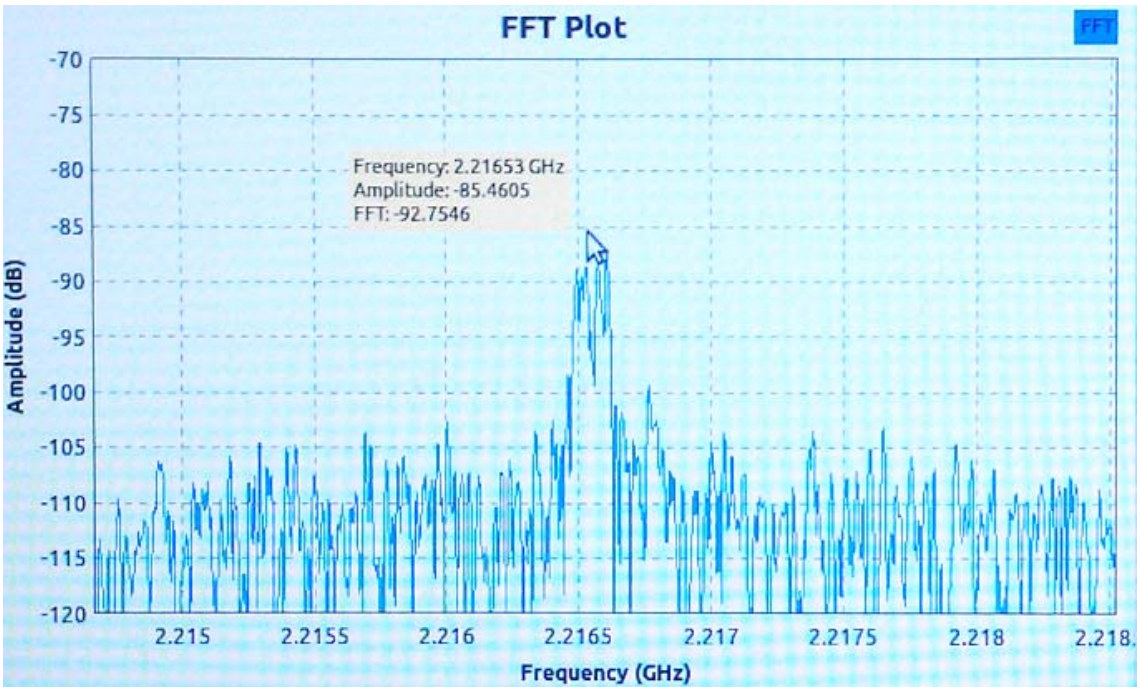


Figure 21. FFT plot of first pass of SCaN Testbed on January 22, 2014

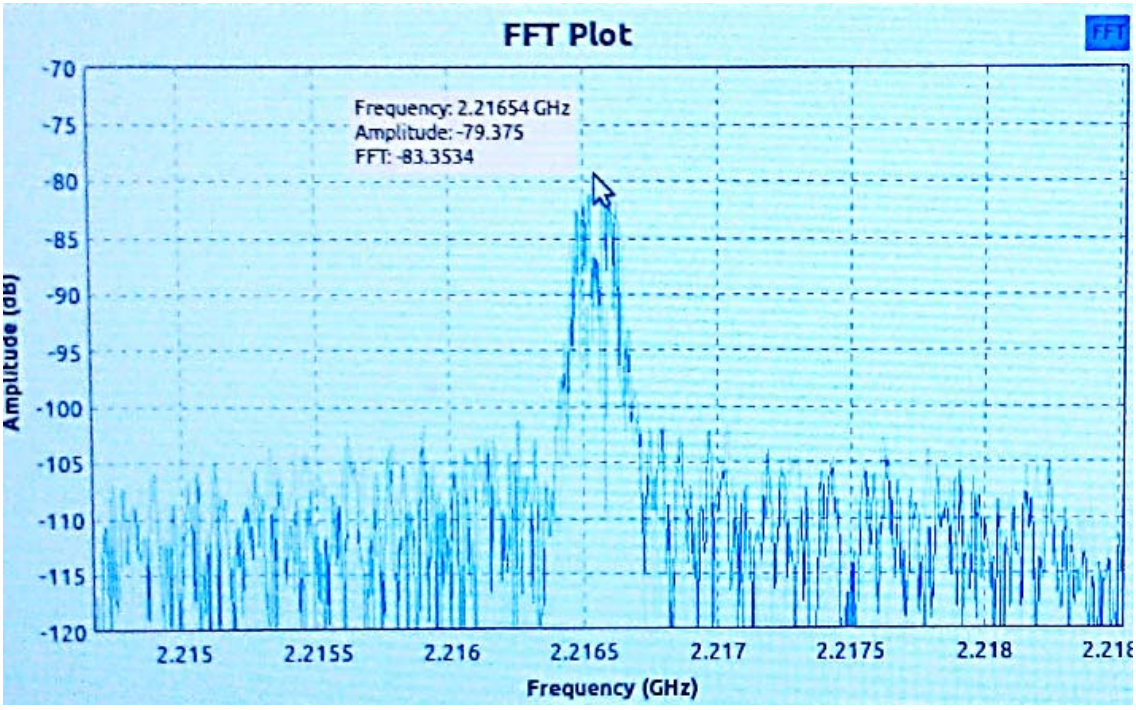


Figure 22. FFT Plot of second pass of SCaN Testbed on January 22, 2014

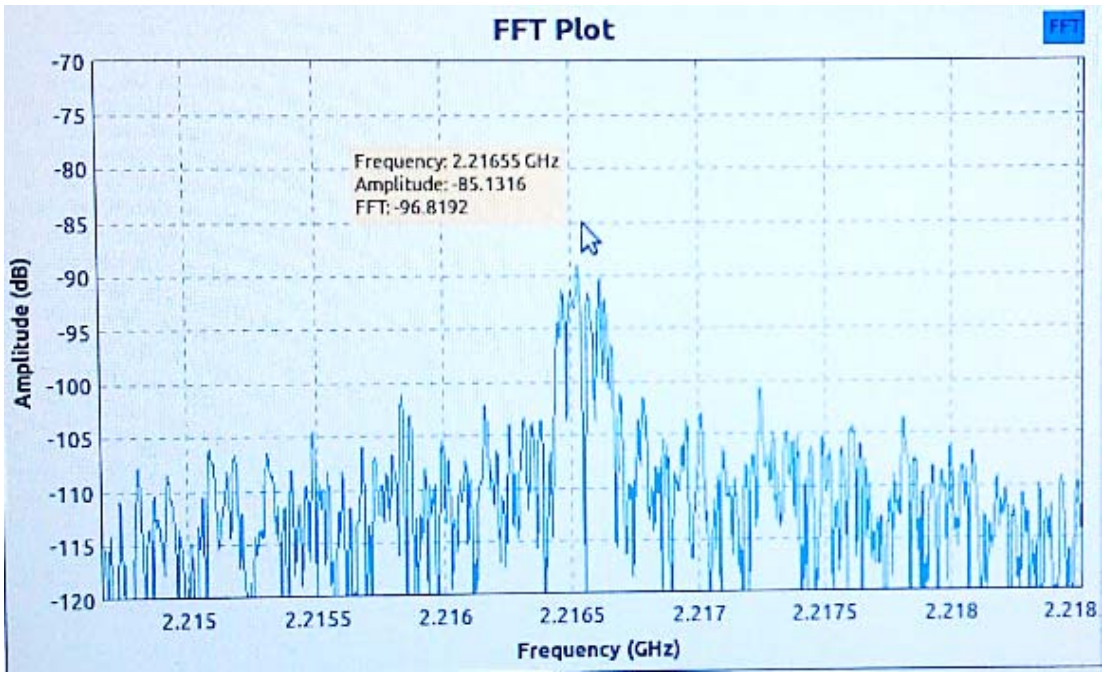


Figure 23. FFT plot of SCaN contact on January 24, 2014

The success of the last five passes verifies the ability of the dish assembly to point accurately, track a moving spacecraft, and receive a signal transmitted from low Earth orbit (LEO).

## D. HAB TEST WITH UHF FEED MODIFICATION OF DISH SYSTEM

### 1. Directed Study

In January 2014, the SmallSat Lab decided to conduct functionality testing on the Colony II Bus (C2B) Kevin Brown Radio (KBR). A HAB test was planned with the primary purpose of validating the ability of the KBR to communicate with the MC3 ground stations at near orbital range. The secondary purpose of the test was to support this thesis by attempting to operate the MC3 3-meter dish antenna at a frequency of 915 MHz, well below its normal S-band operating frequencies.

To accomplish these tests, SmallSat engineers, along with an NPS directed-study student team, designed a unique HAB payload that incorporated a

KBR. The team also designed several unique supporting payload components and software that allowed each component to communicate through the appropriate channels.

This thesis focuses on two aspects of the HAB experiment: the modification of the MC3 parabolic dish feed horn, and the communication operations of the flight. This thesis only gives an overview of the directed study experiment as a whole but, full examination of the HAB flight can be read in the *High Altitude Balloon (HAB) Experiment 2014* [11] report, which was created by the directed study team, including this author.

## 2. Components of the HAB Payload

The NPS SmallSat Lab supplied most of the HAB structural and payload components. These include:

- Fuselage (cardboard rocket body)
- C2B KBR
- Beagle-Bone Black (BBB) Single Board Computer
- Circuit board with radio mount
- Global Positioning System (GPS) (GT-320FW) receivers (x2)
- Automatic Packet Reporting System (APRS)
- Satellite Position and Tracking (SPOT)
- Temperature/humidity data logger (RHTemp101A)
- Battery packs
- Wiring harnesses, connectors and supplemental hardware

Five components used in this research project were specially designed by NPS students. Components include:

- Dual-frequency QHA (415 MHz and 915 MHz)
- Balloon release mechanism (BRM) for flight termination
- Universal UHF antenna feed (915 MHz)
- Universal UHF Antenna Feed Mounting Bracket
- Thermistor based HAB payload component temperature monitoring system

### *a. BBB Single Board Computer*

For this HAB experiment, four components were connected to the BBB UARTs: one GPS receiver, the KBR, the APRS, and the BRM. Python code was developed by SmallSat Lab personnel to control all BBB functions.

The BBB was a critical payload component and a single point of failure. A malfunctioning BBB would prevent the KBR from transmitting. Furthermore, without the BBB flight termination could not be initiated via the BRM, one of the objectives of the HAB flight.

### *b. GPS Receivers*

Two GPS receivers were incorporated into this HAB payload. One receiver provided position data to the APRS. The other receiver provided position data to the BBB. The BBB formatted the GPS data into NMEA packets and sent them to the KBR. Then, those packets were transmitted, via the 915 MHz antenna, to the MC3 ground station.

### *c. Automatic Packet Reporting System*

The Automatic Packet Reporting System (APRS) transceiver, Figure 24, has its own power source and antenna. Three APRS transceivers were employed during HAB flight operations. One APRS transceiver was incorporated into the HAB payload with the primary purpose of transmitting location data to be used for tracking and recovery of the payload. Two other APRS transceivers were located in HAB chase vehicles for use as a redundant measure for sending the command to terminate flight operations via the BRM.

Figure 24. APRS transceiver

### *d. SPOT Tracker*

Several SPOT trackers were used during HAB flight operations. One SPOT Tracker was incorporated into the HAB payload and two were used in chase vehicles.

## 3. Component Interaction

Figure 25 is a conceptual diagram of HAB component interactions with one another and the respective ground stations. The blocks in tan and blue represent HAB payload components. The blocks in green represent components located at the MC3 or in the chase vehicles. Not depicted is the Stanford Research Institute (SRI) 60 foot dish antenna, which also served as a ground component for this HAB flight.

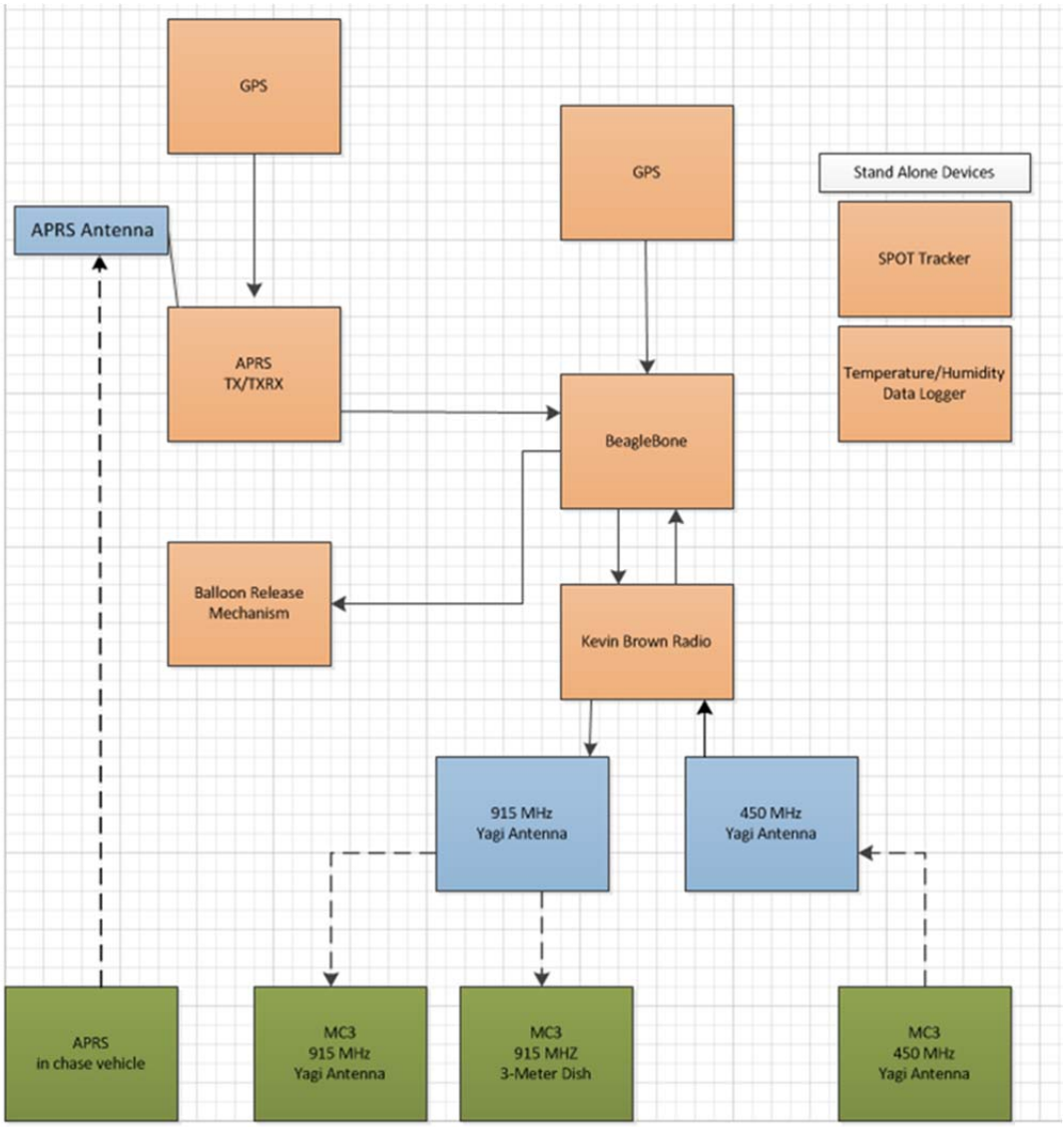


Figure 25. Conceptual diagram of HAB component interaction

## 4. Communication Operations

HAB payload components capable of transmitting and receiving data included the KBR and the APRS transceiver. Additionally, the SPOT tracker was a transmit-only component.

The MC3 ground station at NPS utilized the 450 MHz Yagi antenna for transmissions to the HAB. Receive-only operations were carried out by the 915 MHz Yagi antenna and UHF-enabled 3-meter dish system. Additionally,

transmissions were possible through APRS transceivers located in chase vehicles. Finally, the 60-foot dish located at the Stanford Research Institute was connected to a 915 MHz feed and GDP receiver for receive-only operations. The original plan proposed that transmission would be attempted from the SRI dish antenna, if possible.

To validate the functionality of KBR components the CONOPS called for the KBR to transmit GPS and temperature data continually throughout the flight. This information would be sent every 30 seconds below an altitude of 2000 feet and every two minutes above an altitude of 2000 feet. On occasion, during the flight, the MC3 ground station would be employed to transmit a large packet of information to the KBR. The KBR would then relay that same packet of information back to the MC3 ground station. Successful receipt of the transmitted information at the ground station would confirm that the KBR operated as intended. Furthermore, once an altitude of 80,000 feet was reached, or at the discretion of the HAB flight coordinator, the primary command to release the balloon via the BRM would be sent via MC3.

Transmissions from the balloon, not directed to the MC3 ground station, included the APRS transceiver and the SPOT tracker. Each of these components would transmit GPS position information using its own antenna to its own supporting network throughout the HAB flight. This information would allow HAB team members to track the balloon during flight operations by referencing their respective websites. The data used from these websites is accessible in the *High Altitude Balloon (HAB) Experiment 2014* [11] report.

## 5. 3-Meter Dish Modification

### *a. Creation of the UHF Feed*

The author designed a left hand circular polarization (LHCP) single helical antenna to feed the MC3, 3-meter, parabolic S-band dish. Two design criteria were desired for this antenna: positive gain and a low standing wave ratio (SWR) at 915 MHz. A positive gain on the feed antenna could increase the overall

performance of the dish antenna. Also, the lower the SWR “the more the antenna is matched to the transmission line and the more power is delivered to the antenna. The minimum VSWR is 1.0. In this case, no power is reflected from the antenna, which is ideal” [21].

The design process began with calculating the dimensions of the antenna through the following website: http://www.jcoppens.com/ant/helix/calc.en.php [16]. The dimensions were then taken from the website and entered into 4NEC2 modeling software [17]. This modeling software produced performance charts and a simulated 3-dimensional (3D) object of the antenna. Finally, a physical antenna was constructed from the 4NEC2 model and tested via a spectrum analyzer. Over the course of the design process several models were created in the 4NEC2 software and two physical antennas were created. The following paragraphs describe the design, performance, construction, and testing results of the two physical antennas.

Differing antenna designs were experimented with in the 4NEC2 software to obtain the highest performing 915 MHz antenna. Initially, the performance charts output from the software indicated that a high performing 915 MHz antenna could be created using 900 MHz design parameters, therefore, a physical antenna with those dimensions was created. Table 7 displays the design parameters entered into the *Helix Antenna* website to create the first physical antenna:

- Design frequency: 900 MHz
- Number of turns: 5
- Turn spacing: 0.08 wavelengths

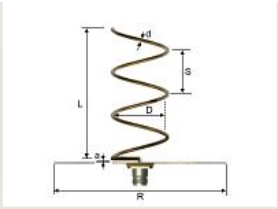

Legend. The letters in the image are used in the table below.

To get a large version, click on the image.

| | | |
|---|---|---|
| Wavelength | | 333.3 mm |
| Ideal diameter (internal) | **D=** | 113.1 mm |
| Gain | | 11.73 dBi |
| Conductor diameter | **d=** | 6.6 mm |
| Winding step (between centers) | **S=** | 26.6 mm |
| Separation of the adapter section | **a=** | 3.2 mm |
| Total conductor length | | 1781.6 mm |
| Minimum reflector diameter | **R=** | 206.6 mm |
| Total antenna length | **L=** | 133.3 mm |

**Design performance**

| | | |
|---|---|---|
| Bandwidth (@ -1dB) | Fmax/Fmin: | 1.06 |
| | Fmax: | 929.52 MHz |
| | Fmin: | 871.41 MHz |
| Bandwidth (@ -3dB) | Fmax/Fmin: | 1.2 |
| | Fmax: | 988.33 MHz |
| | Fmin: | 819.56 MHz |
| Beam width (@ -3dB) | | 82.2 degrees |

Table 7. First UHF helical antenna design details from jcoppens.com

Next, 4NEC2 software was used by the author to model the antenna in free-space and analyze its performance. The graph in Figure 26 is one of the performance charts output from the 4NEC2 modeling software. It displays the gain of the antenna in 2-dimensions. The maximum gain of 9.78 decibels isotropic circular (dBic) is obtained when the signal is received directly down the boresight of the antenna. The graph also displays the gain of the antenna for LHCP (the red line) and right hand circular polarization (RHCP) (the blue line). Figure 26 also displays a 3D image of the antenna. Table 8 summarizes the design values that were input in the 4NEC2 software and the resulting performance in gain and SWR of the antenna. Figure 27 is the graph of the SWR. The yellow line marks the lowest point of the curve, which is at 915 MHz

frequency. The SWR value for 915 MHz is 1.11. These design parameters meet the antenna goal of possessing positive gain and a low SWR value at 915 MHz.

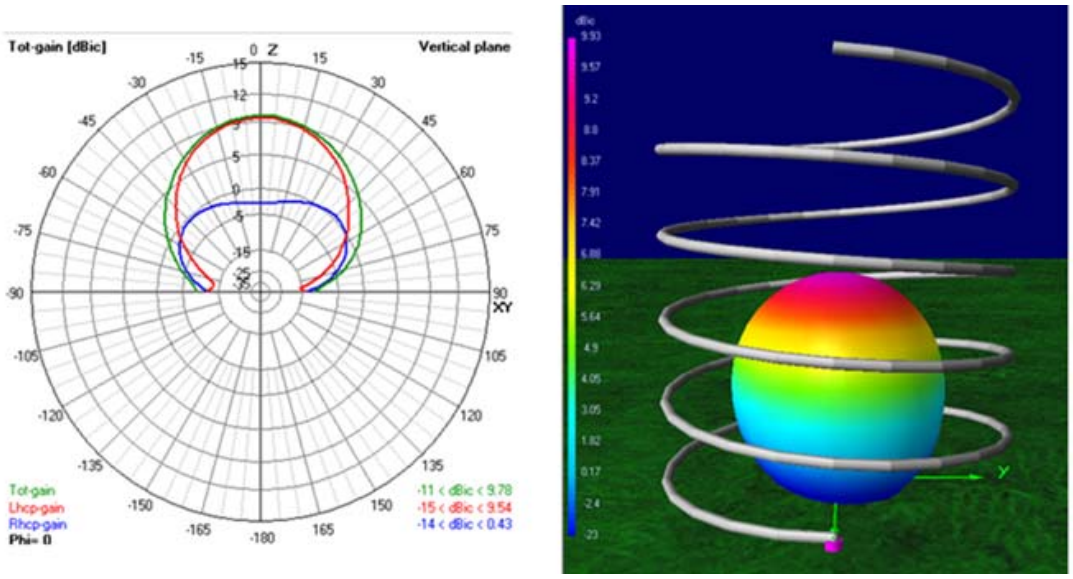


Figure 26. First 915 MHz single helix antenna, 4NEC2 model

| Input Data | | | 915 Single Helix Results | | |
|---|---|---|---|---|---|
| Design Frequency | 900 | Mhz | Total Gain @ nadir | 9.78 | dBic |
| Number of Turns | 5 | λ | Lhcp Gain | 9.54 | dBic |
| Antenna Height | 133.3 | mm | Rhcp Gain | 0.43 | dBic |
| Coil Radius | 56.55 | mm | SWR (50 ohm) | 1.11 | |
| Manual Wire Radius | 1.65 | mm | | | |

Table 8. Design performance of first 915 MHz antenna

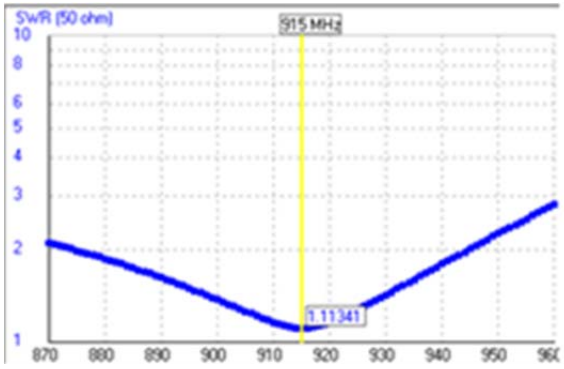


Figure 27. SWR graph of first 915 MHz antenna

Lab personnel used the measurements of the 4NEC2 model to design a three-dimensional (3D) form, which was printed using the SmallSat Lab's 3D printer. A metal reflecting surface was utilized to mount the form. Then a conducting wire was wrapped into the form and soldered into place. Finally, physical testing and verification of the antenna performance was conducted by the author with support from SmallSat personnel using a spectrum analyzer. The first antenna design did not function as expected during live testing. The SWR value at 915 MHz was 2.9 and the SWR at 925 MHz was 1.5. The exact reason for the poor performance at 915 MHz is unknown. Therefore, another iteration of the design process was attempted by the author, this time 915 MHz and 3 turns were used to create the dimensions of the antenna.

The following information was entered into the *Helix Antenna* website to create the final dimensions of the antenna, which are displayed in Table 9:

- Design frequency: 915 MHz
- Number of turns: 3
- Turn spacing: 0.08 wavelengths

| | | |
|---|---|---|
| Wavelength | | 327.8 mm |
| Ideal diameter (internal) | **D=** | 110.6 mm |
| Gain | | 8.6 dBi |
| Conductor diameter | **d=** | 6.5 mm |
| Winding step (between centers) | **S=** | 26.2 mm |
| Separation of the adapter section | **a=** | 3.1 mm |
| Total conductor length | | 1045.5 mm |
| Minimum reflector diameter | **R=** | 203.2 mm |
| Total antenna length | **L=** | 78.6 mm |

**Design performance**

| | | |
|---|---|---|
| Bandwidth (@ -1dB) | Fmax/Fmin: | 1.09 |
| | Fmax: | 957.17 MHz |
| | Fmin: | 874.68 MHz |
| Bandwidth (@ -3dB) | Fmax/Fmin: | 1.38 |
| | Fmax: | 1076.18 MHz |
| | Fmin: | 777.95 MHz |
| Beam width (@ -3dB) | | 106.1 degrees |

Table 9. Final UHF helical antenna design details, from [16]

The graph in Figure 28 displays the gain of the antenna in 2-dimensions. The maximum gain of 9.63 dBic is obtained when the signal is received directly down the boresight of the antenna. The graph also displays the gain of the antenna for LHCP (the red line) and RHCP (the blue line). Table 10 summarizes the design values that were input in the 4NEC2 software and the resulting performance in gain and SWR of the antenna. Figure 29 is the graph of the SWR. The yellow line marks the lowest point of the curve, which is at 919 MHz frequency. The SWR value for 915 MHz is 1.11. These design parameters meet the antenna goal of possessing positive gain and a low SWR value at 915 MHz.

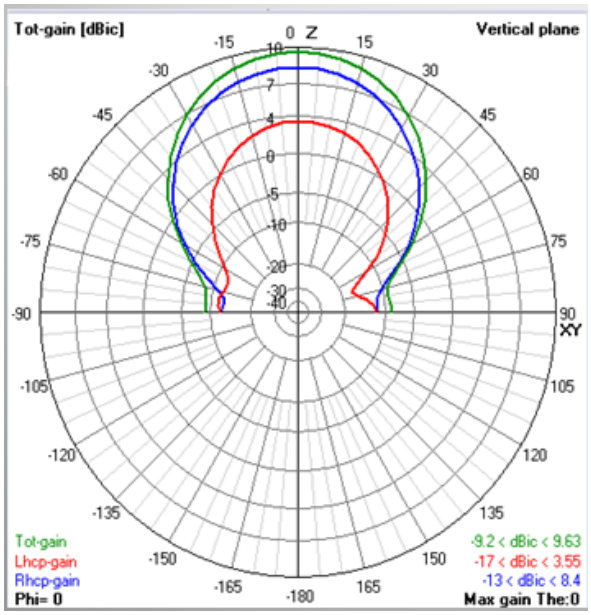


Figure 28. 915 MHz single helix antenna, 4NEC2 model

| Input Data | | | 915 Single Helix | Results | |
|---|---|---|---|---|---|
| Design Frequency | 915 | Mhz | Total Gain @ nadir | 9.63 | dBic |
| Number of Turns | 3 | | Lhcp Gain | 3.55 | dBic |
| Antenna Height | 78.6 | mm | Rhcp Gain | 8.4 | dBic |
| Coil Radius | 55.3 | mm | SWR (50 ohm) | 1.11 | |
| Manual Wire Radius | 1.65 | mm | | | |

Table 10. Final 915 MHz antenna design parameters and results

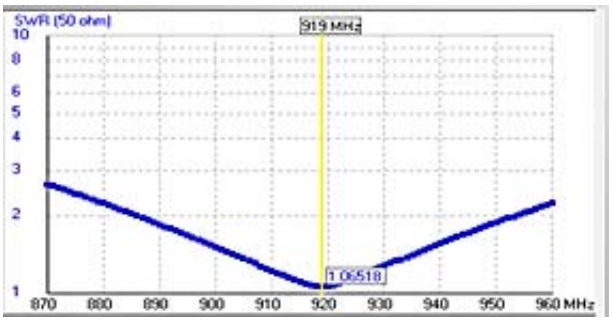


Figure 29. SWR graph of final 915 MHz antenna

To create the physical antenna, lab personnel used the measurements from the 4NEC2 model to design an antenna form to be printed using the SmallSat Lab's 3D printer. Then a metal reflecting surface was utilized to mount the 3D-printed form. Next, a conducting wire was wrapped into the form and soldered into place. Finally, physical testing and verification of the antenna performance was conducted by the author with support from SmallSat personnel using a spectrum analyzer. Figure 30 displays the finished antenna, along with the form, and the metal backplate.

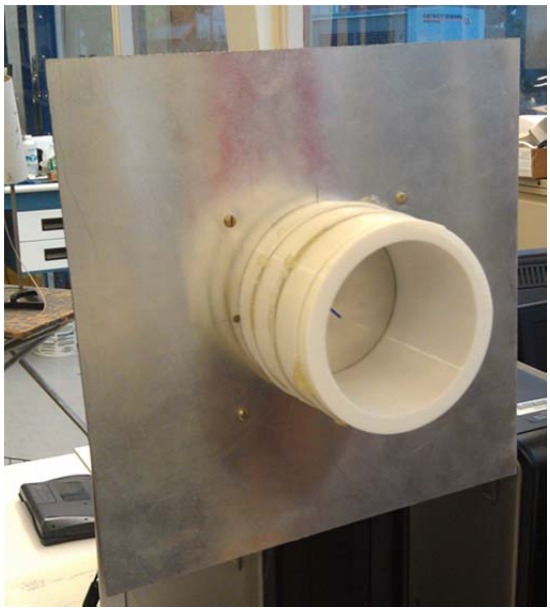

Figure 30. 915 MHz antenna feed for 3-meter parabolic dish

The result of testing conducted by the author using a spectrum analyzer and the antenna is displayed in Figure 31. The spectrum analyzer was set to have a frequency span of 500 MHz. The center of the screen and the lowest point of the center line is at 915 MHz. The SWR value at that point is 1.681. An antenna with an SWR value of 1.6 will have 4.0 percent of the power reflected. The modelled antenna, with an SWR value of 1.1, would have 1 percent of the power reflected. Even though the physical antenna's SWR reflects 3 percent more power than the modelled antenna, the results were still low enough to meet the design requirements.

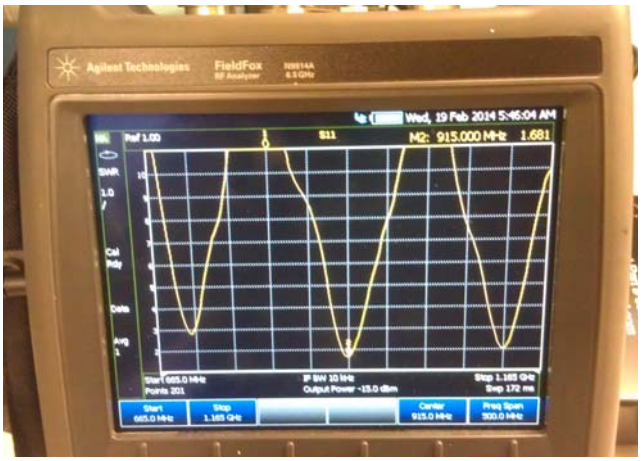


Figure 31. Spectrum analyzer test of final UHF feed antenna

## 6. Flight Path Predication

The online resources and precautions used in Chapter III, Section B were employed to predict the flight path of this HAB experiment. The day prior to launch on March 13, 2014, the websites were referenced and a launch site south of Merced, CA was chosen. The predicted flight path is shown in on the left side of Figure 32. The actual flight path of the HAB is displayed on the right side of Figure 32.

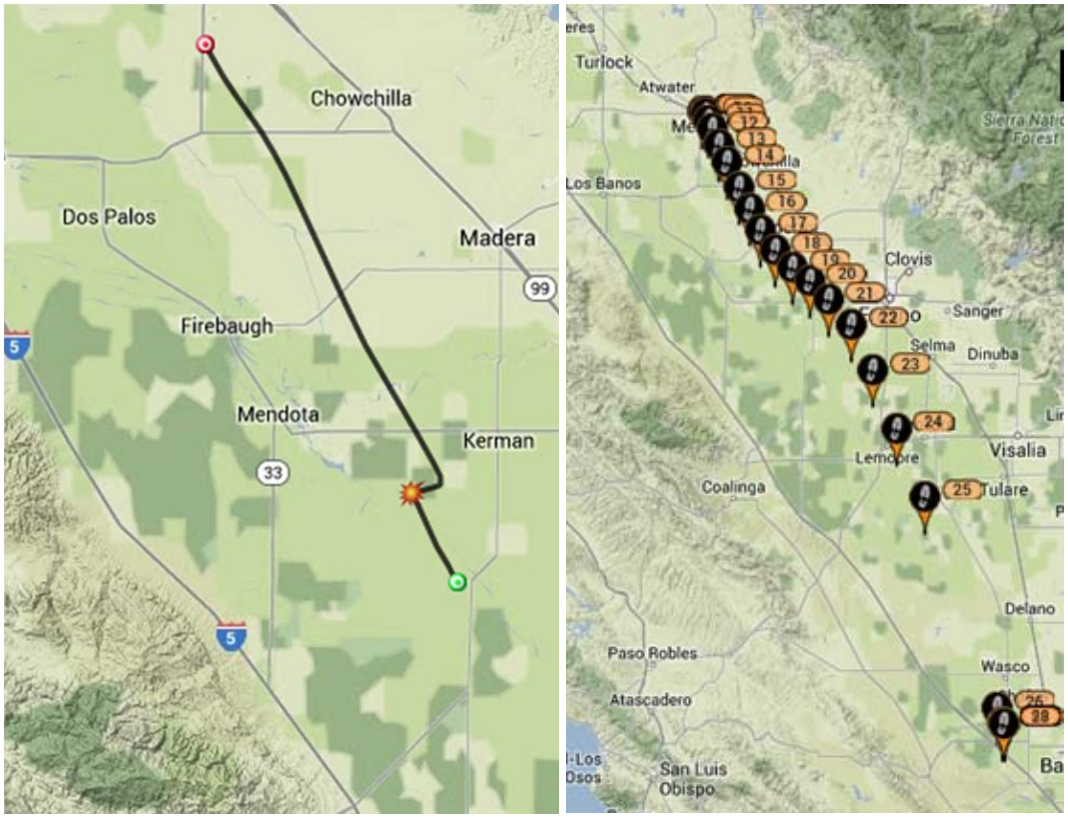


Figure 32. Predicted and actual flight path of directed study HAB, from [11]

## 7. Procedure for Communications

To execute communication operations for the HAB flight, the following time periods were planned for each antenna:

- 1000–1100 MC3 450 MHz Yagi and 915 MHz Yagi will conduct transmit and receive operations with the HAB
- 1100–1115 SRI dish antenna will attempt to transmit to the HAB
- 1100–1130 MC3 dish antenna will conduct receive-only operations
- 1130–1200 MC3 450 MHz Yagi and 915 MHz Yagi will conduct transmit and receive operations with the HAB

Of note, the feed from the MC3 915 MHz Yagi antenna and the modified 3-meter dish system were connected to the GDP for this HAB flight. The GDP can only receive data from one UHF source at a time. Also, the 60 foot antenna at SRI was used periodically during the HAB flight to listen for transmissions from the HAB experiment.

Throughout the flight, the communications plan called for the HAB to transmit GPS and temperature data. Then, if possible, the MC3 ground station would send a large packet of information to the HAB, which would be repeated back to the ground station. All antennas planned to share transmit/receive time as outlined above. At a designated altitude, the MC3 ground station would send a command to release the balloon from the payload. If the balloon failed to release, the command would be given from the APRS transceiver in a chase vehicle. All data sent and received would be recorded along with pertinent information such as signal strength.

## 8. Results

Limited data was received from this HAB flight largely due to two factors. First, the HAB climbed at a slower rate than predicted. Consequently, the mountain range in between the HAB and the MC3 ground station blocked communications for an extended amount of time. Secondly, for a period of the flight, the MC3 ground station personnel were unable to accurately point the dish assembly because faulty GPS data was being transmitted via the APRS and KBR. GPS and APRS data are the primary references that enable MC3 personnel to point the dish at HAB in flight.

Despite the two limiting factors, information transmitted from the KBR was received by the 915 MHz Yagi antenna, the 3-meter dish antenna, and the SRI 60 ft. antenna. The intermittent downlinks between the HAB and the MC3 antennas were recorded through the GDP. Table 11 and Table 12 are taken from the *High Altitude Balloon Experiment 2014* report; they display the measurements from the strongest signals received by the dish assembly and the UHF Yagi antenna. Table 11 and Table 12 are organized by signal strength, with the highest signal strength received at the top of the table. The strongest signal received from the dish assembly, -78 dB, is weaker than the strongest signal received through the MC3 Yagi antenna, -69 dB. This is likely due to the fact that

the dish antenna has a narrow beam width, three degrees full width at -3 dB, and was pointed with marginal accuracy; whereas the Yagi has a much broader beam width, 28 degrees.

| Time (UTC) | Frequency Deviation | Signal (dB) | Bit Synch Deviation | EB/N0 |
|---|---|---|---|---|
| 19:19:47.442 | 2683 | -78 | 4 | 4.8 |
| 19:19:47.976 | 2531 | -78 | 3 | 5.2 |
| 19:19:49.044 | 2370 | -78 | 6 | 5.7 |
| 19:19:49.178 | 2352 | -78 | 5 | 5.7 |
| 19:19:49.311 | 2344 | -78 | 6 | 5.7 |
| 19:19:49.444 | 2334 | -78 | 5 | 5.8 |
| 19:19:49.578 | 2313 | -78 | 5 | 5.7 |
| 19:19:49.711 | 2305 | -78 | 4 | 5.7 |
| 19:20:24.146 | -1811 | -78 | 16 | -1.3 |
| 19:20:24.279 | -1558 | -78 | 15 | -0.5 |

Table 11. NPS 3-meter dish GDP measurements, from [11]

| Time (UTC) | Frequency Deviation | Signal (dB) | Bit Synch Deviation | EB/N0 |
|---|---|---|---|---|
| 19:06:47.412 | 644 | -69 | 10 | 6.8 |
| 19:06:26.986 | 2922 | -70 | 7 | 3.2 |
| 19:06:27.253 | 2802 | -70 | 6 | 4.2 |
| 19:06:27.386 | 2768 | -70 | 5 | 4.4 |
| 19:06:47.145 | 313 | -70 | 10 | 6.9 |
| 19:06:47.278 | 431 | -70 | 11 | 6.8 |
| 19:06:27.521 | 2732 | -71 | 5 | 4.7 |
| 19:06:47.545 | 747 | -72 | 10 | 6.8 |
| 19:06:26.852 | 2971 | -73 | 8 | 3.1 |
| 19:06:27.119 | 2881 | -73 | 6 | 4.1 |

Table 12. NPS MC3 Yagi antenna GDP measurements, from [11]

Overall, the UHF feed on the dish antenna was successfully employed. It received several packets of information from the KBR at a near orbital range. This shows that it is feasible to design and build an operational UHF antenna feed. It also validates the fact that the 3-meter dish can be operated at 915

MHz,well outside of its normal operating range. Further testing should be done to determine whether the dish antenna with UHF feed has higher or lower capability than the MC3 Yagi antenna.

## E. SUMMARY

Chapter III discussed local hilltop testing with the MHX-2400 radio, communications testing with NASA's SCaN Testbed and the two HAB experiments that were conducted in support of this thesis and their individual results. The tests were conducted to examine the dish system's ability to accurately point at and track a moving target, then maintain a link and receive data. Chapter IV discusses the conclusions and future work to be done with regards to the 3-meter dish assembly.

# IV. CONCLUSION AND FUTURE WORK

## A. CONCLUSION

This thesis has documented the installation and calibration of the dish assembly. Through the installation process, limitations created by the surrounding terrain and the keyhole constraint were identified. NPS was able to save thousands of dollars by using SmallSat lab personnel to install the antenna and using an existing antenna mount already available on campus. During the calibration process, the dish assembly was rebalanced and subsequently the slew rate of the dish was increased.

The capabilities of the 3-meter dish assembly have been verified through testing. The four experiments discussed in this thesis validate the capability of the dish system to accurately point, track a moving target, create a link and receive data via S-band and UHF frequencies. The UHF feed antenna designed for the dish system and optimized for 915 MHz successfully received data from the KBR on a high altitude balloon at near orbital distances. Therefore, it is possible for the dish assembly to be used outside of its normal operating range.

The dish assembly is expected to be a great benefit to the NPS MC3 ground station. It should have a higher gain, better pointing accuracy and faster slew rates than the Yagi antennas [6]. Also, it is possible for the dish assembly to be used as the primary UHF antenna for MC3 nodes if future tests are successful. Therefore, it is recommended that dish assemblies become an integral part of all future MC3 nodes for use at 915 MHz as well as for the S-band frequencies. Dish systems come in a variety of styles at varying price ranges. Ideally, a dish that does not have a keyhole constraint should be considered by new MC3 nodes, if the budget permits.

## B. FUTURE WORK

### 1. Keyhole Constraint

The keyhole constraint causes communication time to be lost during spacecraft passes. Currently, there are changes that can be made to the dish assembly to overcome the 90 degree elevation keyhole. The changes involve limit switches that are incorporated into the hardware and software of the dish assembly. Engineers at M2 Antenna Systems should be consulted when exploring these changes. In regards to the azimuth keyhole constraint, an analysis involving the pros and cons of physically turning the dish assembly to alter where the keyhole begins should be completed.

### 2. UHF Feed on Dish Assembly

The data that was received from the the KBR on the HAB through the UHF feed on the dish assembly was limited. During the time periods where data was received, the UHF Yagi antenna outperformed the dish assembly. Therefore, further testing should be done to validate the performance of the UHF feed. Further testing of the UHF feed assembly could be done from local hilltops, with HAB tests, or with operational spacecraft.

### 3. Performance Characteristics

The experiments performed in this thesis were limited to receive only operations. Permission to transmit from the dish assembly should be pursued. After approval is received, tests involving HABs, the SCaN testbed, or other operational satellites should be done to validate transmission performance of the dish assembly.

To further characterize the performance of the dish assembly, a signal strength graph should be created. The experiment could involve taking an S-band and UHF radio to a location that is at zero degrees elevation in regard to the dish assembly and slowly turning the dish 360 degrees while recording signal strength.

## 4. Summary

This thesis helps move the MC3 project forward. In particular, this thesis helps further the understanding of the MC3 S-band dish for future S-band capable CubeSats. It may even be able to support the expected C2B CubeSats operating at 915 MHz. It will be exciting to test the capabilities of the 3-meter dish as soon as working C2Bs are launched and operating in space.

THIS PAGE INTENTIONALLY LEFT BLANK

# APPENDIX A. MHX TEST MESSAGES

Below is the entire text for Test 1. (44 characters total)

----Test 1----

Test 1
Test 1
Test 1
Test 1
Test 1

Below is the entire text for Test 2. (150 characters total)

---- Test 2 -----

Test 3 Test 2
Test 4 Test 2
Test 5 Test 2
Test 6 Test 2
Test 7 Test 2
Test 8 Test 2
Test 9 Test 2
Test 10 Test 2
Test 11 Test 2
Test 12 Test 2

The first four lines of Test 3 are displayed below. The message begins with a line of dashes and the title of the test message. Following the title line is a blank line and 20 lines of text that repeat “Test 3” 10 times on each line. There are 1,449 characters in this message.

----------Test 3----------

Test 3 Test 3 Test 3 Test 3 Test 3 Test 3 Test 3 Test 3 Test 3 Test 3
Test 3 Test 3 Test 3 Test 3 Test 3 Test 3 Test 3 Test 3 Test 3 Test 3
...
...
... (20 lines total)

Test 4 is partially displayed below. The message begins with a line of dashes and the title of the test message. Then one blank line follows. Next, there are 100 lines of text that repeat “Test 4” 10 times on each line. Preceding every group of 10 lines there is a line of dashes that are numbered 1 through 10. There are 7,670 characters in this test message.

----------Test 4----------

-1----------
Test 4 Test 4 Test 4 Test 4 Test 4 Test 4 Test 4 Test 4 Test 4 Test 4
Test 4 Test 4 Test 4 Test 4 Test 4 Test 4 Test 4 Test 4 Test 4 Test 4
...
...
... (10 lines total in this block)

-2----------
Test 4 Test 4 Test 4 Test 4 Test 4 Test 4 Test 4 Test 4 Test 4 Test 4
Test 4 Test 4 Test 4 Test 4 Test 4 Test 4 Test 4 Test 4 Test 4 Test 4
...
...
... (repeats for a total of 10 blocks)

# APPENDIX B. HAB MHX-2400 MESSAGES RECEIVED BY 3-METER DISH FROM 20:09 TO 20:13 ON DECEMBER 21, 2013

Below is an excerpt from the data log of the directed study HAB flight. Each line of data begins with the time in seconds, followed by the date and time in UTC. Next is the type of data that is being logged. The information preceded by the words “data from MHX =” are packets of information received from the HAB MHX radio. After a packet of information is successfully received from the HAB the data is processed into an easy to read format and used to steer the 3-meter dish.

1387656587.9, 2013-12-21 20-09-47 [UTC], Data from MHX = <>
1387656593.9, 2013-12-21 20-09-53 [UTC], Data from MHX =
<$GPGGA,195544.00,3706.7269,N,12015.71570,36,06,47,292,40*76>
1387656598.9, 2013-12-21 20-09-58 [UTC], Data from MHX = <>
1387656606.9, 2013-12-21 20-10-06 [UTC], Data from MHX =
<$GPGGA,195556.00,3706.7366,N,12015.7180,W,1,10,01.0,00094.5,M,-028.7,M,,*52>
1387656606.9, 2013-12-21 20-10-06 [UTC], Blat=37.112277 [deg], Blon=-120.261967 [deg], Balt =94.500000 [m]
1387656606.9, 2013-12-21 20-10-06 [UTC], M2_Thread::placing new position: AZ=67.67, EL=0.02
1387656606.9, 2013-12-21 20-10-06 [UTC], Az=67.7 deg, El=0.0 deg, Dist=96.1 mile, Dist=154.6 km
1387656647.1, 2013-12-21 20-10-47 [UTC], RSSI = -102 dBm
1387656648.1, 2013-12-21 20-10-48 [UTC], Data from MHX = <ATA>
1387656648.1, 2013-12-21 20-10-48 [UTC], Data from MHX = <>
1387656705.3, 2013-12-21 20-11-45 [UTC], OK
OK
1387656724.1, 2013-12-21 20-12-04 [UTC], Data from MHX = <>
1387656759.5, 2013-12-21 20-12-39 [UTC], OK
OK
1387656765.3, 2013-12-21 20-12-45 [UTC], Data from MHX = <>
1387656775.3, 2013-12-21 20-12-55 [UTC], Data from MHX =
<$GPGGA,195838.00,3706.7104,N,12015.6683,W,1,10,01.0,00944.4,M,-028.7,M,,*51>
1387656775.3, 2013-12-21 20-12-55 [UTC], Blat=37.111840 [deg], Blon=-120.261138 [deg], Balt =4267.200000 [m]
1387656775.3, 2013-12-21 20-12-55 [UTC], M2_Thread::placing new position: AZ=67.70, EL=1.56
1387656775.3, 2013-12-21 20-12-55 [UTC], Az=67.7 deg, El=1.6 deg, Dist=96.1 mile, Dist=154.6 km
1387656775.5, 2013-12-21 20-12-55 [UTC], OK
1387656789.8, 2013-12-21 20-13-09 [UTC], OK
OK
1387656796.6, 2013-12-21 20-13-16 [UTC], Data from MHX = <>
1387656806.6, 2013-12-21 20-13-26 [UTC], Data from MHX = <>
1387656822.6, 2013-12-21 20-13-42 [UTC], Data from MHX = <>
1387656830.6, 2013-12-21 20-13-50 [UTC], Data from MHX =
<$GPGGA,195935.00,3706.3413,N,12015.5336,W,1,10,01.0,01255.2,M,-028.7,M,,*5E>
1387656830.6, 2013-12-21 20-13-50 [UTC], Blat=37.105688 [deg], Blon=-120.258893 [deg], Balt =1255.200000 [m]
1387656830.6, 2013-12-21 20-13-50 [UTC], M2_Thread::placing new position: AZ=67.96, EL=1.56
1387656830.6, 2013-12-21 20-13-50 [UTC], Az=68.0 deg, El=1.6 deg, Dist=96.0 mile, Dist=154.6 km
1387656830.9, 2013-12-21 20-13-50 [UTC], OK

THIS PAGE INTENTIONALLY LEFT BLANK

# LIST OF REFERENCES


[1] A. Mehrparvar. (2014, February 20). *CubeSat Design Specification*. [Online]. Available: http://www.cubesat.org/images/developers/cds_rev13_final.pdf

[2] G. Minelli, A. Felt, D. Rigmaiden, J. Horning and J. Newman, “Mobile CubeSat command and control (MC3) ground stations,” PowerPoint presentation, SSAG, Naval Postgraduate School, Monterey, CA, 2014.

[3] C. LeGaux, “STARE CubeSat communication testing simulation and analysis,” M.S. thesis, SSAG, Naval Postgraduate School, Monterey, CA, 2012.

[4] P. B. Ibbitson, “Mobile CubeSat command and control architecture and CONOPS,” M.S. thesis, SSAG, Naval Postgraduate School, Monterey, CA, 2012.

[5] R. Griffith, “Mobile CubeSat command and control,” M.S. thesis, SSAG, Naval Postgraduate School, Monterey, CA, 2011.

[6] Microhard Systems Inc. *MHX-2400 OEM Industrial Wireless Modem*. [Online]. Available: http://www.microhardcorp.com/pdf/MHX2400.pdf

[7] *MHX-2400 Operating Manual: 2.4GHz Spread Spectrum OEM Transceiver*, Revision 1.56. Calgary, Alberta: Microhard Systems Inc., 1985, pp. 1, 35, 46.

[8] R. Jenkins, “NPS-SCAT systems engineering and payload subsystem design, integration, and testing of NPS' first CubeSat,” M.S. thesis, SSAG, Naval Postgraduate School, Monterey, CA, 2010.

[9] A. Bein, “NPS-SCAT (Solar Cell Array Tester), the construction of NPS’ first prototype CubeSat,” M.S. thesis, SSAG, Naval Postgraduate School, Monterey, CA, 2008.

[10] Radio Regulations Articles, International Telecommunication Union, Geneva, Switzerland, 2012, pp. 261.

[11] S. Alcaide, D. Donaldson, P. Schrafft, C. Jarolimek, and A. Felt, “High altitude balloon (HAB) experiment 2014,” Naval Postgraduate School, Monterey, CA, 2014.

[12] *SCaN Testbed Project GRC-CONN-DOC-5022 Rev A*. Lewis Field, OH: NASA, John H. Glenn Research Center, 2012, pp. 4–17.

[13] N. Nogueira, “Project Stratosphere proposal,” PowerPoint presentation, SSAG, Naval Postgraduate School, Monterey, CA, 2013.

[14] APRS. Aprs.fi. [Online]. Available: http://aprs.fi

[15] SPOT. Spot ready for adventure. [Online]. Available: https://login.findmespot.com/spot-main-web/auth/login.html

[16] John Coppens. Helix antenna. [Online]. Available: http://www.jcoppens.com/ant/helix/calc.en.php

[17] A. Voors. (2014 March 28). NEC based antenna modeler and optimizer (4NEC2). [Online]. Available: http://www.qsl.net/4nec2

[18] HABHUB Website. Habhub. [Online]. Available: http://habhub.org

[19] Ettus. Ettus Research: A National Instruments Company. [Online]. Available: https://www.ettus.com/product/details/UN210-KIT

[20] J. Wertz, D. Everett, and J. Puschell, *Space Mission Engineering: The New SMAD*. Hawthorne, CA: Microsm Press, 2011. p. 635.

[21] Antenna Theory. VSWR. [Online]. Available: http://www.antenna-theory.com/definitions/vswr.php

# INITIAL DISTRIBUTION LIST

1. Defense Technical Information Center
   Ft. Belvoir, Virginia

2. Dudley Knox Library
   Naval Postgraduate School
   Monterey, California